AD_____

Award Number: W81XWH-08-1-0164

TITLE: The Genomic Actions and Functional Implications of Nuclear PRLr in Human Breast Carcinoma

PRINCIPAL INVESTIGATOR: Alyson Fiorillo

CONTRACTING ORGANIZATION: Northwestern University
Evanston, IL 60208

REPORT DATE: March 2011

TYPE OF REPORT: Annual Summary

PREPARED FOR: U.S. Army Medical Research and Materiel Command
Fort Detrick, Maryland 21702-5012

REPORT DOCUMENTATION PAGE

Form Approved
OMB No. 0704-0188

1. REPORT DATE *(DD-MM-YYYY)*	**2. REPORT TYPE**	**3. DATES COVERED** *(From - To)*
01-03-2011	Annual Summary	1 MAR 2008 - 28 FEB 2011

4. TITLE AND SUBTITLE
The Genomic Actions and Functional Implications of Nuclear PRLr in Human Breast Carcinoma

5a. CONTRACT NUMBER

5b. GRANT NUMBER
W81XWH-08-1-0164

5c. PROGRAM ELEMENT NUMBER

6. AUTHOR(S)
Alyson Fiorillo

E-Mail: a-fiorillo@md.northwestern.edu

5d. PROJECT NUMBER

5e. TASK NUMBER

5f. WORK UNIT NUMBER

7. PERFORMING ORGANIZATION NAME(S) AND ADDRESS(ES)
Northwestern University
Evanston, IL 60208

8. PERFORMING ORGANIZATION REPORT NUMBER

9. SPONSORING / MONITORING AGENCY NAME(S) AND ADDRESS(ES)
U.S. Army Medical Research and Materiel Command
Fort Detrick, Maryland 21702-5012

10. SPONSOR/MONITOR'S ACRONYM(S)

11. SPONSOR/MONITOR'S REPORT NUMBER(S)

12. DISTRIBUTION / AVAILABILITY STATEMENT
Approved for public release; distribution unlimited

13. SUPPLEMENTARY NOTES

14. ABSTRACT

The direct actions of transmembrane receptors within the nucleus remain enigmatic. In this report we demonstrate that the prolactin receptor (PRLr) localizes to the nucleus where it functions as a co-activator through its interactions with the latent transcription factor Stat5a and the high mobility group N2 protein (HMGN2). We identify a novel transactivation domain within the PRLr that is activated by ligand-induced phosphorylation, an event coupled to HMGN2 binding. The association of the PRLr with HMGN2 enables Stat5a-responsive promoter binding, thus facilitating transcriptional activation and promoting anchorage-independent growth. We propose that HMGN2 serves as a critical regulatory factor in Stat5a-driven gene expression by facilitating the assembly of PRLr/Stat5a onto chromatin, and that these events may serve to promote biological events that contribute to a tumorigenic phenotype. Our data imply that phosphorylation may be the molecular switch that activates a cell surface receptor transactivation domain, enabling it to tether chromatin-modifying factors, such as HMGN2, to target promoter regions in a sequence-specific manner.

15. SUBJECT TERMS
Prolactin prolactin receptor, Sta5a, breast cancer

16. SECURITY CLASSIFICATION OF:			**17. LIMITATION OF ABSTRACT**	**18. NUMBER OF PAGES**	**19a. NAME OF RESPONSIBLE PERSON**
a. REPORT	**b. ABSTRACT**	**c. THIS PAGE**			USAMRMC
U	U	U	UU	55	**19b. TELEPHONE NUMBER** *(include area code)*

Standard Form 298 (Rev. 8-98)
Prescribed by ANSI Std. Z39.18

Table of Contents

Part 1 - Introduction

The role of the polypeptide hormone prolactin (PRL) in the pathogenesis and progression of human breast cancer has become established in recent years. Acting at the autocrine/paracrine level, PRL functions to stimulate the growth and motility of human breast cancer cells. These actions require the presence of the transmembrane prolactin receptor (PRLr). The classic belief is that the PRLr functions "at a distance" through the activation of signaling networks. However, numerous reports now indicate that intact transmembrane receptors localize to the nucleus and directly contribute to transcriptional activation. Yet, without DNA binding capabilities or intrinsic chromatin remodeling activity, the mechanism by which these receptors serve to regulate transcription remains elusive. In this thesis, we investigate the function of nuclear PRLr, given preliminary observations of its nuclear presence. For the first time, we find that the prolactin receptor (PRLr) localizes to the nucleus where it functions as a co-activator through interaction with the latent transcription factor Stat5a and the high mobility group N2 protein (HMGN2). We identify a novel transactivation domain (TAD) within the PRLr and demonstrate that it is activated by ligand-induced phosphorylation, an event coupled to HMGN2 binding. Depletion of HMGN2 reduces binding of PRLr and Stat5a to chromatin, and results in impaired Stat5a-drive gene expression. We propose that the PRLr-mediated recruitment of HMGN2 facilitates PRLr/Stat5a assembly onto chromatin, thus enabling Stat5a-driven transcription. These data are of significant importance to the broad field of signal transduction as they expand the growing field of cell surface receptor nuclear localization to include a novel receptor. In addition, these studies are of note as they elucidate a molecular mechanism though which cell surface receptor-mediated transcriptional regulation is achieved. A direct pathophysiologic relevance is demonstrated through observations that the PRLr TAD is necessary for *in vitro* anchorage-independent growth and is increasingly activated as a function of neoplastic progression *in vivo* Our data, encompassing the mechanistic, functional and biological actions of nuclear PRLr, provide key insights into full-length cell surface receptor nuclear translocation, a phenomenon that has remained elusive for nearly two decades.

Part 2 – Proposed Aims

Three specific aims were proposed in this pre-doctoral award.

Specific Aims
(1) Evaluate the function of the PRLr as a potential transcription factor and/or Stat5a co-activator.
(2) Determine the molecular mechanism of PRLr nuclear localization.
(3) Analyze the role of nuclear PRLr in the pathogenesis of human breast carcinoma.

Part 3 - Statement of Work

The tasks to achieve the specific aims above are covered in the statement of work as outlined below. Completed idems of the proposal are **indicated in bold.**

Specific Aim 1. **Evaluate the function of the PRLr as a potential transcription factor and/or Stat5a co-activator (Months 1-20):**

Experiment 1.1 – What domains of PRLr are necessary and sufficient for transactivation?

a. **Months 1-4: Construct Gal4-PRLr truncation mutants to elucidate the transactivation domain of PRLr**
b. **Months 4-7: Perform luciferase experiments with constructs in 293, MCF7 and T47D cells**
c. **Months 7-12 Fine map the transactivation domain of the PRLr.**

The above data were reported in the 2009 and 2010 Summary of Work. These data are also included in the attached paper.

Experiment 1.2 - Does PRLr bind DNA in a Stat5a independent manner?

a. Months 6-7: Acquire biotinylated probes for EMSA
b. Months 7-8: Perform EMSA studies using nuclear extracts
c. Months : 8-10: Perform *in vitro* transcription/translation of PRLr and Stat5a
d. Months 10-20: Perform EMSA studies on using *in vitro* transcribed/translated proteins

We have identified that the chromatin modifying protein, HMGN2 binds to both the PRLr transactivation domain, and Stat5a. We therefore performed experiments that ask the question: What is the role of HMGN2 in Stat5a driven gene expression? These questions have be investigated and are presented in the attached paper.

Specific Aim 2. **Determine the molecular mechanism of PRLr nuclear localization (Months 1-24):**

Experiment 2.1 - Does PRLr sequence KPKK facilitate PRLr and Stat5a nuclear localization though a "classic" nuclear import pathway?

a. **Months 1-4: Construct muPRLr (KPKK mutation) construct**
b. **Months 4-8: Perform transfections of wt and mutant PRLr constructs in CHO cells**
c. **Months 4-8: Perform western blots on cytoplasmic and nuclear extracts of CHO transfectants**

We have performed these experiments which were reported last year, but have since seen that mutation of the PRLr NLS has no effect of its nuclear localization. However, we have also identified two specific residues that are necessary for PRLr transactivation function. Therefore, we are utilizing a PRLr transactivation deficient construct to ask the question: What are the mechanistic and functional effects of mutation of the PRLr transactivation domain?

Experiment 2.2 - Is Jak2 tyrosine kinase necessary for initiating PRLr nuclear localization?

a. Month 8: Acquire Jak2 inhibitor (AG-490) and Jak2 siRNA
b. Months 9-10: Perform drug treatment and on T47D cells
c. Months 9-10: Perform western blot analysis on T47D nuclear and cytoplasmic lysates
   -Probe for PRLr, controls
d. Months 10-12: Optimize si-RNA knockdown of Jak2
e. Months 12-14: Perform western blot analysis of T47D cells with Jak2 knockdown
   -Probe for PRLr, controls

We have chosen to hold off on these experiments so that we can explore other aims more rigorously.

***Experiment 2.3 - Is nuclear PRLr derived from the cell surface*?**

a. Months 14-16: Optimize biotinylation conditions
b. Months 16-24: Perform biotinylation experiments in nuclear/cytoplasmic lysates.

These results were reported in the 2009/2010 Summary of work and are presented in the attached paper.

Specific Aim 3. **Analyze the role of nuclear PRLr in the pathogenesis of human breast carcinoma (Months 12-36):**

Experiment 3.1 – Does nuclear targeted PRLr have the ability to induce neoplastic abnormalities in vitro?

a. Months 12-16: Create lentiviral constructs
b. Months 16-20: Create stable cell lines
c. Months 20-24: Perform 3-D matrigel assay
d. Months 22-24: Perform proliferation assay
e. Months 24-28: Perform Growth on soft agar assay

We have identified the PRLr transactivation domain and HMGN2, the protein that is recruited to the PRLr transactivation domain, and is involved in chromatin regulation. We have therefore generated the following cells lines to study functional effects:

1. **PRLr knockdown**
2. **wt PRLr overexpression**
3. **transactivation-deficient PRLr overexpression (PRLr Y406F/D411A)**

As the PRLr knockdown shRNA targets the 3'UTR, we are created rescue cells lines:
1.PRLr knockdown, wt PRLr overexpression
2. PRLr knockdown, Y406FD411A overexpression

We have also investigated the role of the PRLr TAD in neoplastic progression in vivo. Results are experiments are detailed in Part 4.

Part 4 - Results

4.1 Specific Aim 1. *Evaluate the function of the PRLr as a potential transcription factor and/or Stat5a co-activator.*

4.1.1 Mutation of the PRLr TAD results in reduced Stat5a-mediated gene expression, but does not affect cell surface signaling

We previously demonstrated that PRLr residues Y406/D411 are critical for PRLr-specific transactivation (DOD Summary 2010). To determine the importance of these residues in Stat5a-mediated gene expression, we contructed MCF7 stable cell lines expressing Empty vector, PRLr or PRLr with Y406F/D411A mutation, (herein referred to as PRLrYDmut). Indeed, mutation of the PRLr TAD prevents PRL stimulation Stat5a-mediated *CISH* transcription (**Figure 4A**). To demonstrate that TAD mutation did not affect cell surface signaling we determined the ability of PRLrYDmut to bind to and activate Stat5a. Subsequently, western blot and co-immunoprecipitation analyses, demonstrated that PRLrYDmut did not have significant defects in cell surface signaling, thus demonstrating its role specifically in the nucleus (**Figure 4B,C**).

4.1.2 The PRLr TAD is phosphorylated in a PRL-dependent manner

Residue Y406 within the PRLr TAD is proposed to be a putative phosphorylation site, so we next investigated its phosphorylation status in response to PRL. Indeed, using a phospho-specific antibody we found that Y406 phosphorylation occurred in a PRL-induced manner (**Figure 4D, E**). Additionally we found that this Y406 phosphorylated-PRLr is seen almost exclusively in nucleus, further supporting its role in nuclear PRLr-specific transactivation (**Figure 4F**).

4.1.3 The PRLr transactivation domain, but not the transactivation mutant binds to HMGN2

We sought to confirm that HMGN2 the yeast-two hybrid findings – that HMGN2 binds to the PRLr and specifically, binds to its TAD. To do this, we utilized MCF7 stable cell lines expressing Empty vector, PRLr or transactivation-deficient PRLrYDmut. Co-Immunoprecipitation results revealed that HMGN2 binds to wtPRLr but not PRLrYDmut in a PRL-dependent manner. (See Appendix, **Figure 5A,B**).

4.1.4 HMGN2 but not HMGN1 is necessary for PRL-induced Stat5a-mediated transcription

Previously (reported in DOD Summary 2010), we constructed T47D stable knockdown cell lines using an shRNA targeting HMGN2, or a non-silencing shRNA. Using these cell lines we analyzed PRL-induced *CISH* transcription. HMGN2 depletion resulted in a significant decrease in PRL-induced CISH expression (**Figure 5E**). This was further confirmed using an HMGN2 construct that lacked the ability to bind to nucleosomes (**Figure 5F**). An siRNA targeting HMGN1, however, yielded no significant effect (**Figure S4E, F**). Thus, these data demonstrate the importance of HMGN2 on PRL-induced Stat5a-mediated gene expression.

4.1.5 HMGN2 is necessary for PRLr and Stat5a assembly onto chromatin

We previously found that HMGN2 is bound to the PRLr/Stat5a chromatin complex on the *CISH* promoter (DOD Summary 2010). Given the putative role of HMGN2 in chromatin remodeling/unfolding, we hypothesized that HMGN2 may be important in promoting the binding of PRLr/Stat5a to chromatin. Indeed, depletion of HMGN2 significantly decreased the binding of both the PRLr and Stat5a to the *CISH* promoter (**Figure 6A, B**). These results suggest that HMGN2 play a crucial role in the activation of PRL-induced gene expression, in part, by facilitating the assembly of PRLr/Stat5a onto chromatin.

4.2 Specific Aim 3 – Analyze the role of nuclear PRLr in the pathogenesis of human breast carcinoma.

4.2.1 PRLr, but not PRLrYDmut, promotes soft agar colony growth in vitro

Given the association of the PRLr and its ligand in the pathogenesis of breast cancer we sought to elucidate the functional effects of PRLr transactivation activity. Soft agar growth of cells was quantified to determine if the transactivation function of nuclear PRLr was relevant to tumorigenic growth *in vitro.* Parental MCF10AΔp53 cells formed only a small number of colonies, consistent with previous reports (38). Expression of PRLr but not expression of PRLrYDmut significantly augmented colony formation (**Figure 7A, B**). These results imply that an activated PRLr TAD may be required in order for PRLr to promote a transformed phenotype.

4.2.2 Translational implications of Nuclear PRLr

The above data has demonstrated that one of the critical residues in PRLr transactivation, Y406, is phosphorylated. A phospho-specific antibody was therefore developed against Y406 to determine where this phosphorylation might occur, and how this phosphorylation might be related to breast cancer progression. To determine the relationship between PRLr Y406 phosphorylation and neoplastic progression, we performed microscopic evaluation of immunohistochemistry (IHC) on a progression breast tissue microarray (TMA).

The TMA consisted of 12 patient-matched normal, tumor and lymph node metastasis breast tissue samples from ER+/Her- patients as well as 8 patient-matched normal, tumor and lymph node metastasis and 8 patient-matched normal and tumor samples. Additionally the array included 4 non-matched tumor samples from ER-/Her2- patients. PRLr Y406 phosphorylation was primarily observed in the nucleus of tissue samples, consistent with the hypothesis that phosphorylation activates the nuclear function of the PRLr. Visual scoring of PRLr Y406 phosphorylation revealed a significant increase specifically in nuclear intensity of primary breast tumor and in lymph node metastasis samples in comparison to normal samples (**Figure A**). This data suggests that phosphorylation of Y406 may be crucial for PRLr transactivation, and may initiate or contribute to a tumorigenic phenotype.

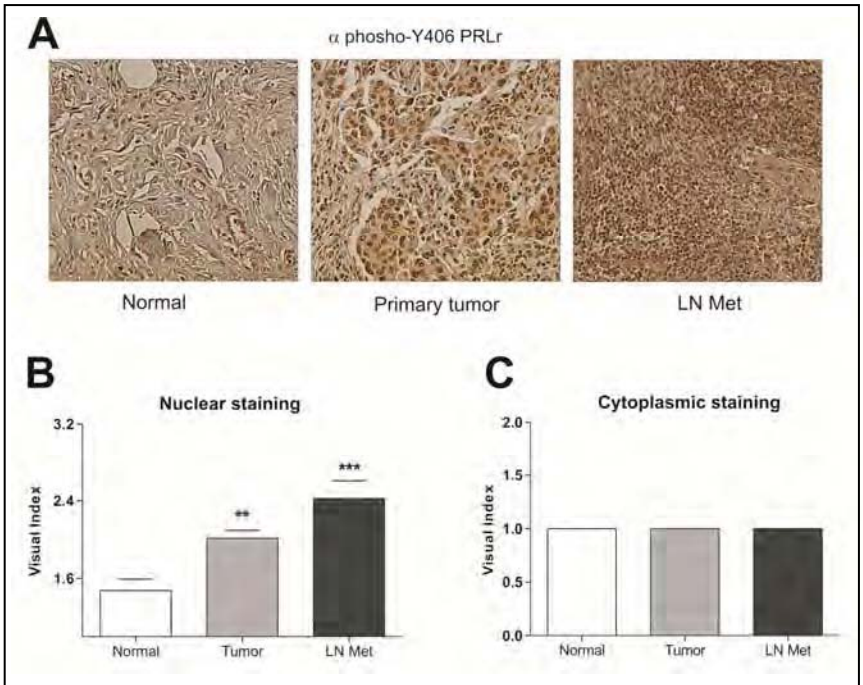

Figure A.The PRLr TAD phosphorylation is increased as a function of neoplastic progression. (**A)** Representative anti-phosphoY406 PRLr IHC from matched normal, primary tumor and lymph node metastasis breast tissue. The photomicrograph demonstrates the observed increase in PRLr Y406 phosphorylation in malignant tissues, with accumulation in the cell nucleus. Magnification = original ×40. **(B)** Quantification of nuclear PRLr Y406 phosphorylation. **(C)** Quantification of cytoplasmic PRLr Y406 phosphorylation The results are shown as the mean ± SEM. Normal, normal breast tissue; Tumor, primary breast tumor; LN Met, Lymph Node Metastasis; IHC, immunhistochemistry; **, p<0.01; ***, p<0.001.

Part 5 - Key Research Accomplishments

- Identification of critical residues in the PRLr transactivation domain
- Verification that HMGN2 binds to the PRLr and is recruited to the CISH promoter upon PRL stimulation
- Cloning of several retroviral constructs, and development of expertise in retroviral transduction
- Providing key insight into the role of the PRLr as a transcriptional coactivator
- Providing evidence for the mechanism of PRLr nuclear localization
- Development of presentation skills through numerous departmental and cancer center wide talks
- Development of collaboration skills by learning techniques perfected by adjacent laboratories
- Development of mentor skills by assisting in colleagues paper revisions and by teaching new techniques
- Submission of a manuscript to Molecular Endocrinology
- Completion of thesis

Part 6 - Reportable Outcomes

6.1 Publications:

- **Fiorillo, Alyson A.**, Medler, Terry R., Feeney, Yvonne B., Gadd, Liu, Yi, Tommerdahl, Kalie L. and Clevenger, Charles, V. *Molecular Endocrinology. 2011* "The prolactin receptor transactivation domain binds HMGN2 to regulate Stat5a-driven gene expression*." Submitted.*

- **Fiorillo, Alyson A.,** Feeney, Yvonne B., Medler, Terry R., Tommerdahl, Kalie L., Clevenger, Charles V. *American Journal of Pathology. 2011* "The PRLr transactivation domain contributes to *ER*α and *PR* transcription and is associated with malignant progression." *In preparation.*

- Zheng, Jiamao, **Fiorillo, Alyson A**., Medler, Terry R., Feng, Fang, Clevenger, Charles, V. *Journal of Biological Chemistry*. 2010 "Negative cross-talk between NFAT1 and STAT5 signaling in breast cancer". *In Revision*

- Fang F, Zheng J, Galbaugh T, **Fiorillo A**, Hjort E, Zeng X, Clevenger C. *J. Molecular Endocrinology. 2010* "Cyclophilin B as a co-regulator of prolactin-induced gene expression and function in breast cancer cells."

6.2 Selected Poster Presentation and Abstracts (5 of 15)

- Cancer Center Retreat (2010) Northwestern University
  Alyson A. Fiorillo, Samantha L. Gadd, Feng Fang, Yvonne Feeney, Kalie Tommerdahl and Charles V. Clevenger. *"Ligand induced phosphorylation of the PRLr activates its transactivation activity through interaction with the chromatin modifying protein, HMGN2."*

- AACR Annual Meeting (2009) Denver, CO
  Alyson A. Fiorillo, Samantha L. Gadd, Feng Fang and Charles V. Clevenger. *"Nuclear PRLr Functions as a Transcriptional Activator"*

- Endocrine Society Meeting (2008) San Francisco, CA (Invited Poster Competition)
  Alyson A. Fiorillo, Samantha L. Gadd, Feng Fang and Charles V. Clevenger. *"The Role of Nuclear Prolactin Receptor as a Transcriptional Activator."*

- Northwestern University, Lewis Lansberg Research Symposium (2008) Chicago, IL
  Alyson A. Fiorillo, Samantha L. Gadd, Feng Fang and Charles V. Clevenger. *"The Role of Nuclear Prolactin Receptor as a Transcriptional Activator."*

- Gordon Research Conferences, Prolactin/Growth Hormone (2008) Ventura Beach, CA
  Alyson A. Fiorillo, Samantha L. Gadd, Feng Fang and Charles V. Clevenger. *"The Role of Nuclear Prolactin Receptor as a Transcriptional Activator."*

Part 7 - Conclusions

The central goal of this grant was to determine the role ofh PRLr in the nucleus. In this body of work, we have demonstrated the novel intranuclear actions of the PRLr as a Stat5a co-activator and as such, have provided a more complete understanding of the complex nature of PRLr signaling. The data within herein provides key mechanistic insight into the phenomenon of transcriptional regulation of cell surface receptors by demonstrating that the plasma membrane-bound prolactin receptor (PRLr) localizes to the nucleus and activates Stat5a-driven transcription by mediating the temporal recruitment of HMGN2, a factor involved in chromatin modulation and transcriptional activation. A functional TAD within the PRLr is necessary for this transcriptional activation; its phosphorylation may serve as the initiation factor that triggers conversion of a cell surface receptor to a nuclear co-activator. Our proposed model is one in which 1) PRLr-mediated recruitment of HMGN2 facilitates the association of PRLr and Stat5a with the *CISH* proximal promoter and 2) the coordinated assembly of the HMGN2/ Stat5a/ PRLr complex onto chromatin initiates *CISH* transcriptional activation. HMGN2 is known to promote transcription, yet it possesses no DNA sequence specificity. Thus, our data also imply that the PRLr may function as the required adapter protein that tethers HMGN2 to promoter regions in a sequence-specific manner. These data also provide a plausible solution to the conundrum of how differential gene expression profiles are conferred by cell surface receptors that activate converging pathways. Hung and coworkers have demonstrated the pathological nature of nuclear EGFr, as well as therapeutic strategies that would harness the knowledge of nuclear EGFr action in cancer. Preliminary studies have demonstrated the potential value of nuclear PRLr as a novel biomarker. The development of a strategy to target the nuclear-only functions of the PRLr while leaving its cell surface function intact could therefore be of therapeutic value. It would also be conceivable to exploit the outside-in function of the PRLr as a therapeutic strategy since it is well know that the PRLr is expressed in the majority of breast tumors. One possible scenario would be to conjugate a DNA-damaging agent to PRL, and allow it to "piggyback" into the nucleus with the PRLr. There is already at least one successful effort to use nuclear EGFr as a means of introducing Auger-electron-emitting ^{111}In-radiolabelled hEGF into the nucleus, to promote tumor cell death (Wang et al 2001). However, before these types of clinical applications can be pursed with nuclear PRLr, larger cohorts of breast cancer specimens must be examined to conclusively demonstrate a positive correlation between nuclear PRLr and breast cancer pathogenesis. Nevertheless, the work presented here certainly yields implications for the function of cell surface receptors in normal cellular processes and malignant progression.

Part 8 – Appendices

8.1 Manuscript submitted to Molecular Endocrinology: HMGN2 binds a novel transactivation domain in nuclear-localized PRLr to coordinate Stat5a-mediated transcription

Alyson A. Fiorillo[1], Terry R. Medler[1], Yvonne B. Feeney[1], Yi Liu[1], Kalie L. Tommerdahl[1] and Charles V. Clevenger[1*]

[1]Breast Cancer Program, Robert H. Lurie Comprehensive Cancer Center & Department of Pathology
Northwestern University, Chicago, Illinois USA

Abbreviated Title: PRLr/HMGN2 regulate Stat5a-driven transcription

Key words: Nuclear-localized cell surface receptor/HMGN2/PRLr/transcriptional regulation/signal transduction

***Corresponding Author:**
Charles V. Clevenger, M.D. Ph.D.
Department of Pathology, Northwestern University,
Robert H. Lurie Building 4-107
303 East Superior Street, Chicago, IL 60611 USA
Phone: 312.503.5750
Fax: 312.503.0095
E-mail: clevenger@northwestern.edu

~This work was supported by a DOD BC073401 Pre-doctoral traineeship award

DISCLOSURE STATEMENT: The authors have nothing to disclose

8.1.1 Abstract

The direct actions of transmembrane receptors within the nucleus remain enigmatic. In this report we demonstrate that the prolactin receptor (PRLr) localizes to the nucleus where it functions as a co-activator through its interactions with the latent transcription factor Stat5a and the high mobility group N2 protein (HMGN2). We identify a novel transactivation domain within the PRLr that is activated by ligand-induced phosphorylation, an event coupled to HMGN2 binding. The association of the PRLr with HMGN2 enables Stat5a-responsive promoter binding, thus facilitating transcriptional activation and promoting anchorage-independent growth. We propose that HMGN2 serves as a critical regulatory factor in Stat5a-driven gene expression by facilitating the assembly of PRLr/Stat5a onto chromatin, and that these events may serve to promote biological events that contribute to a tumorigenic phenotype. Our data imply that phosphorylation may be the molecular switch that activates a cell surface receptor transactivation domain, enabling it to tether chromatin-modifying factors, such as HMGN2, to target promoter regions in a sequence-specific manner.

8.1.2 Introduction

In the mammary gland, the signaling cascades induced by the polypeptide hormone prolactin (PRL) require the presence of the cell surface prolactin receptor (PRLr). Studies focusing on PRLr have described its signaling capabilities almost exclusively at the plasma membrane, and have demonstrated that upon ligand binding, the PRLr-associated kinases Jak2, Src, and Tec become activated (1). These kinases in turn activate the transcription factors Stat5a (2) and Elf5 (3) resulting in specific patterns of gene expression. These events are biologically relevant as the PRLr and its downstream signaling components have been implicated in breast cancer pathogenesis. Specifically, the PRLr is overexpressed in breast cancer tissue (4), and its increased stability and resistance to ubiquitin-mediated degradation prolongs its associated signaling events in primary breast tumors (5). Epidemiologically, high PRL serum levels are associated with a two-fold increase in breast cancer risk (6).

The canonical pathway that is activated by PRL-PRLr engagement is Jak2/Stat5a (7). Jak2 is constitutively associated with the PRLr, and is activated by ligand which induces the phosphorylation and activation of Stat5a (8). These events ultimately result in the upregulation of PRL target genes such as *Cyclin D1* (9) and *CISH (Cytokine Inducible SH2-Containing Protein)* (10), whose overexpression in breast cancers has been observed (11).

The Jak2/Stat5a pathway is widely shared with other transmembrane receptors such as epidermal growth factor receptor (EGFR) and growth hormone receptor (GHr); however the mechanism defining the specificity of induced gene expression between these receptor-signaling pathways remains unknown. Interestingly, there have been numerous reports indicating that intact transmembrane receptors localize to the nucleus. These reports include, but are not limited to, members of the ErbB family of receptors (12-16), GHr (17-18), and FGFr (15, 19-22). Additionally, a subset of these studies has demonstrated that nuclear-localized transmembrane receptors contribute to transcriptional activation. Examples include nuclear EGFr-mediated transactivation of *Aurora A*, *iNOS*, and *COX-2* genes (23) (24-25), nuclear FGFr potentiation of c-jun (22) and nuclear GHr-mediated upregulation of *Survivin*, *Mybbp*, and *Dysadherin* (18). Collectively, these observations suggest that the trafficking of a cell surface into the nucleus contributes to transcriptional activation and may serve to impart specific patterns of ligand-induced gene expression. However, the specific mechanism by which intranuclear receptors serve to regulate transcription has not been fully described.

In this study, we demonstrate that PRL initiates PRLr nuclear translocation in mammary epithelial cells *in vitro*, and breast tissue *in vivo*. Furthermore, we identify a novel PRLr transactivation domain (TAD) that upon phosphorylation, recruits the chromatin-modifying protein HMGN2, enabling Stat5a-mediated gene expression. This is

the first report to identify a novel TAD within the PRLr and demonstrate its inducible interaction with a nucleosome-binding protein whose presumed functions are directly related to transcriptional activation.

8.1.3 Results

Intranuclear localization of PRLr

Preliminary observations in our laboratory and others (26-27) led us to hypothesize that the PRLr may localize to the nucleus. Thus, cell fractionation was performed on T47D breast cancer cells, which exhibit high endogenous PRLr levels. Utilizing an antibody specific to the PRLr extraacellular domain, we detected full length PRLr in both non-nuclear and nuclear fractions **(Figure 1A).** The endoplasmic reticulum (ER) membrane protein, calnexin was partitioned to the non-nuclear fraction, demonstrating that detected nuclear PRLr was not the result of contamination from newly-translated ER-localized proteins. Immunoblots were also probed with anti-Lamin B1 to demonstrate nuclear purity. An antibody specific to the PRLr intracellular domain demonstrated similar results **(Figure 1B)** as did transient transfection of epitope-tagged PRLr cDNA in MCF7 breast cancer cells **(Figure S1A)** and CHO cells (**Figure S1-B**). These findings were further confirmed by immunohistochemical analysis of normal and malignant breast tissue samples. In this analysis the nuclear intensity of PRLr in tissue samples was scored from 0 to 3, and a score above 1.5 was counted as positive. Using this method, 12/16 normal breast epithelial samples and 20/35 malignant tissue samples showed positive nuclear staining. Representative pictures from these analyses are shown in **Figure 1C.** A secondary antibody control to demonstrate antibody specificity was performed as shown in **Figure S1C.** Taken together, these results clearly demonstrate that the PRLr is present in the nucleus *in vitro* and *in vivo*.

To determine whether nuclear PRLr was derived from the cell surface or from an independent cytoplasmic pool, biotinyation of T47D cells was used to track the PRLr from the cell surface. After cell fractionation and streptavidin immunoprecipitation, a significant amount of endogenous biotinylated PRLr was detected in the nucleus as a function of PRL stimulation **(Figure 1D)**. These results were specific to the PRLr, as the cell surface receptor, β1 Integrin, despite its ability to be internalized, was not detected in the nucleus. Our results therefore suggest that a significant portion of the PRLr that accumulates in the nucleus is both derived from the cell surface and triggered by ligand stimulation.

Nuclear PRLr activates Stat5a-dependent transcription

Given that Stat5a and PRLr interact at the cell surface in a ligand-dependent manner, we postulated that PRLr/Stat5a may interact in the nucleus. PRLr non-nuclear and nuclear immunoprecipitates in T47D cells were analyzed for Stat5a binding**.** Indeed, a ligand-inducible interaction between the two proteins in the nucleus was observed.

Comparable results were seen when using either anti-PRLr **(Figure 2A)** or anti-Stat5a **(Figure S2A)** as the immunoprecipitating antibody**.**

The finding of an interaction between the PRLr and Stat5a suggested that the two proteins exist in a functionally important nuclear complex. Previous reports have shown that Stat5a binds strongly to GAS elements on the *CISH* proximal promoter after 30 minutes of PRL treatment (28) and were verified here **(Figure S2B).** Thus, we utilized chromatin immunoprecipitation (ChIP) to determine whether nuclear PRLr could also bind to the Stat5a-driven *CISH* proximal promoter (see schematic, **Figure 2B, top**). In untreated T47D cells, an anti-PRLr-ECD antibody precipitated a small but detectable amount of DNA from the *CISH* proximal promoter, while PRL stimulation significanlty enhanced this binding. PRLr promoter occupancy was observed when performing ChIP using an antibody specific to the extracellular domain (ECD) **(Figure 2B, bottom)** or intracellular domain (ICD) **(Figure S2C).** As a control for non-specific DNA binding, it was determined that the PRLr was not significantly enriched a region downstream of the proximal promoter in the *CISH* open reading frame.

Based on the above findings, we hypothesized that nuclear PRLr may function as a Stat5a co-activator, where Stat5a provides the DNA-binding domain that tethers PRLr to chromatin, and PRLr provides a transactivation domain (TAD) to promote transcription. Since knockdown or overexpression of the PRLr would alter its cell surface actions, the C-terminal addition of an SV40 large T antigen nuclear localization signal (NLS) was utilized to force the nuclear localization of the PRLr (termed PRLr-NLS) (**See Schematic Figure 2C, expression via western blot Figure S2D**). Enhanced nuclear localization of each construct was verified by fluorescence microscopy (data not shown). To measure the effects of forced PRLr nuclear localization on Stat5a-regulated gene expression a *CISH* reporter construct was utilized **(Figure 2C)**. Overexpression of wild-type PRLr potentiated reporter activation two-fold, as has been previously reported **(Figure 2D) (**Fang et al., 2008**)**. However, transfection of PRLr-NLS potentiated this effect, thus revealing a significant correlation between PRLr nuclear localization and Stat5a-induced gene expression **(Figure 2D)**.

To further examine this phenomenon, the PRLr intracellular domain (ICD) was fused to an SV-40 NLS and this construct was overexpressed in MCF7 cells **(Figure S2D)**. As NLS-ICD lacks a signal peptide and transmembrane domain and is therefore completely devoid of cell surface signaling capabilities, this approach enabled us to examine the nuclear-only properties of the PRLr. Indeed, forced nuclear localization of the PRLr ICD increased *CISH* reporter activity compared to control, further demonstrating the transcriptional function of nuclear PRLr and suggesting this function resides within the ICD **(Figure 2D)**.

Since the actions of the NLS-ICD construct were enhanced by ligand stimulation, this suggested that Stat5a binding to GAS elements of the *CISH* reporter was required for PRLr-specific transactivation. To test this possibility, the ability of NLS-ICD to activate *CISH* transcription in the presence of a constitutively active Stat5a (Stat5a1*6) was examined. Interestingly, overexpression of Stat5a 1*6 in MDA-231 cells modestly increased reporter activity, while transfection of either wild-type PRLr or NLS-ICD yielded no significant effect. However, the forced nuclear localization of the PRLr-ICD coupled with the expression of constitutively active Stat5a markedly increased reporter activity, therefore suggesting that activated Stat5a is required for PRLr nuclear action **(Figure S2E).**

A novel transactivating domain within PRLr

We hypothesized that the PRLr ICD possessed innate transactivation activity based the ability of Stat5a-mediated gene expression to be induced by the forced nuclear localization of the PRLr ICD. In order to identify the region that may be responsible for transactivation, the PRLr ECD or ICD domains were fused to a Gal4 DNA binding domain (DBD), and a UAS/GAL4-based reporter system was utilized (**Figure 3A**). While Gal4-ICD activated the Gal4-UAS reporter ~300 fold, Gal4-ECD yielded no significant activity **(Figure 3B).** Notably, the transactivation effects observed in the presence of Gal4-ICD were seven-fold higher than Gal4-Stat5aTAD, which was previously demonstrated to be a potent transactivator as measured by the Gal4-UAS system (29).

We next constructed sequential C-terminal truncations of Gal4-ICD to further fine map the PRLr TAD **(Figure 3C, D)**. Using this method, we identified 44 amino acids that were necessary for PRLr transactivation (404-448). Subsequent cross-species DNA analysis highlighted a small region of homology (residues 405-411) in which four residues were highly conserved **(Figure 3E).** To determine which, if any, of these residues were integral in PRLr-specific transactivation, we performed site-directed mutagenesis within the Gal4-404-448 fusion. Interestingly, Y406F or D411A mutations significantly decreased transactivation, while their simultaneous mutation completely ablated transactivation **(Figure 3F)**.

The PRLr TAD is critical for Stat5a-driven transcription

The above data led us to hypothesize that introduction of the transactivation-defective double mutation into full length PRLr (herein referred to as PRLrYDmut), would negatively affect Stat5a-mediated transcription. Thus, stably transfected pools expressing PRLr or PRLrYDmut were generated from parental MCF10AΔp53 cells or MCF7 cells

(Figure S3A,B). MCF10AΔp53 cells were selected for their low level of endogenous PRLr expression and signaling and MCF7 cells for their moderate level of endogenous PRLr expression and signaling. While overexpression of the PRLr significantly enhanced PRL-induced *CISH* mRNA, expression of PRLrYDmut significantly compromised in this effect in both stable cell pools **(Figure 4A, Figure S3D).** Expression of PRLrYDmut also significantly diminished PRL-stimulated *CISH* reporter activity **(Figure S3E).**

To ensure that the effects of PRLr-YDmut expression were not due to deficient cell-surface signaling, the activation of downstream messengers was assessed. Western blot analysis demonstrated the ability of the transactivation-deficient mutant (PRLrYDmut) to induce Stat5a **(Figure 4B),** Akt and Erk phosphorylation **(Figure S3E)**. Moreover, PRLrYDmut retained its ability to bind Stat5a both in the cytoplasm and in the nucleus **(Figure 4C).** Collectively, these data indicate that mutation of the PRLr TAD does not compromise cell surface signaling relevant to the activation of downstream messengers. Therefore, the reduction in PRL-induced *CISH* transcription is specifically due to a defect in the transactivation capabilities of PRLrYDmut.

It was intriguing that one of the conserved residues required for PRLr transactivation was a tyrosine, as TADs are known to be regulated by a variety of post-translational modifications including phosphorylation (30). To determine if PRLr residue Y406 was phosphorylated, we generated a phospho-specific antibody against this residue. Indeed, western blot analysis confirmed that Y406 was rapidly phosphorylated in response to PRL **(Figure 4D).** Immunofluoresence similarly demonstrated inducible Y406 phosphorylation and a significant portion of this phosphorylation was observed in the nucleus (**Figure 4E)**. Immunoprecipitation analysis also revealed the specificity of the newly generated Y406 antibody, as no detectable phosphorylation of Y406 was observed in cells expressing PRLr-YDmut **(Figure 4F)**.

Interaction of PRLr and HMGN2

TADs are known to be responsible for stabilizing transcription factors at specific DNA loci and facilitating the recruitment of transcriptional co-factors (31). Our identification of a novel PRLr TAD led us to hypothesize that, in concert with Stat5a, nuclear PRLr may interact with other proteins involved in transcriptional regulation. A yeast-two-hybrid using the PRLr-ICD as bait was performed previously in our lab to identify potential PRLr binding proteins (32). One of the identified proteins was the high mobility group protein, HMGN2 (Gadd and Clevenger 2006, unpublished data). HMGN2 is known to bind to the nucleosome core particle and induce structural changes in chromatin (33). Interestingly, the intranuclear localization of HMGN2 has been shown to be associated with regions of highly active

transcription (34). Based on this, we postulated that HMGN2 binds to the PRLr TAD and regulates Stat5a-mediated transcription.

To verify yeast-two-hybrid results, the Gal4 system was utilized. HMGN2 and either wild-type or mutant Gal4-PRLr constructs were transfected into cells expressing a stably integrated Gal4-UAS reporter. Co-immunoprecipitation with anti-Gal4 followed by immunoblot analysis demonstrated the association of the PRLr TAD (404-448) and HMGN2, while binding was not observed between HMGN2 and the TAD mutant (Y406FD411A) **(Figure 5A)**, or a domain adjacent to the TAD (data not shown).

To further confirm these results in the full length PRLr, co-immunoprecipitation studies with stably transfected T47D cell pools were performed. PRL stimulated the association of PRLr with HMGN2, while mutation of the TAD (PRLrYDmut) abolished this interaction (**Figure 5B**). Additionally, PRL-induced Y406 phosphorylation was detected in HMGN2 control or wild-type PRLr immunoprecipitates **(Figure 5B).** Co-immunoprecipitation analysis using an anti-V5 antibody further confirmed these findings (data not shown). Collectively, these results demonstrate a ligand-inducible interaction between the PRLr and HMGN2 and indicate that phosphorylation may be the molecular switch that facilitates TAD activation and subsequent HMGN2 recruitment.

We next sought to determine the extent of HMGN2 occupancy at Stat5a-target promoter regions, via ChIP. A PRL-induced association between HMGN2 and the *CISH* proximal promoter region was observed, (**Figure 5C)** further supporting the hypothesis that HMGN2 is a critical factor in facilitating Stat5a-mediated transcription.

The ability of HMGN2 to potentiate the Stat5a-driven transcription was next investigated. HMGN2 overexpression significantly enhanced *CISH* reporter activity, while the combination of PRLr and HMGN2 yielded an additive effect **(Figure 5D).** Furthermore, shRNA-mediated knockdown of HMGN2 impaired PRL-induced *CISH* mRNA **(Figure 5E, knockdown efficiency shown in Figure S4A,B)**. These results were confirmed using siRNA-mediated HMGN2 depletion with a second target sequence (**Figures S4C,D**).

High mobility group family member HMGN1 exhibits high homology and similar function to HMGN2 (35). We therefore performed siRNA-mediated knockdown to determine if HMGN1 also played a role in PRLr-mediated transactivation. However, as shown in **Figures S4E** and **S4F**, HMGN1 knockdown had no effect on *CISH* mRNA levels. To complement siRNA data and to rule out off-target effects, a dominant negative HMGN2 mutant was generated by replacement of two highly conserved serines within the nucleosome binding domain (S24E/S28E, termed NBDmut). Mimicking serine phosphorylation at these sites has been previously shown to prevent HMGN2 chromatin binding (36).

Interesintly, while wild-type HMGN2 overexpression potentiated *CISH* mRNA induction in MCF7 cells, NBDmut expression almost completely prevented this induction **(Figure 5F)** suggesting that the HMGN2 NBD is required for its effects on Stat5a-target gene expression.

Regulation of PRLr and Stat5a promoter engagement by HMGN2

HMGN2 is thought to facilitate chromatin decompaction through its chromatin unfolding domain (37). Based on this, we hypothesized that HMGN2 may enable Stat5a and PRLr promoter binding. To test this, chromatin immunoprecipitation on shHMGN2 or shNS cell pools was performed. As shown in **Figure 6A and B**, knockdown of HMGN2 decreased the relative amount of PRLr and Stat5a bound to the *CISH* promoter by 6-fold and 2-fold, respectively. Taken together, these data indicate that HMGN2 may facilitate recruitment of these factors to the *CISH* promoter and is required for maximal PRL-induced *CISH* transcription.

The PRLr TAD is necessary for a transformed phenotype *in vitro*

Given the association of the PRLr and its ligand in the pathogenesis of breast cancer we sought to elucidate the functional effects of PRLr transactivation activity. Soft agar growth of cells was quantified to determine if the transactivation function of nuclear PRLr was relevant to tumorigenic growth *in vitro.* Parental MCF10AΔp53 cells formed only a small number of colonies, consistent with previous reports (38). Expression of PRLr but not expression of PRLrYDmut significantly augmented colony formation (**Figure 7A, B**). These results imply that an activated PRLr TAD may be required in order for PRLr to promote a transformed phenotype.

8.1.4 Discussion

In this report, we provide strong evidence that in addition to its cell surface signaling functions, the PRLr possesses co-activator function: 1) it localizes to the nucleus, 2) has a defined TAD with potent activity, 3) associates with both the transcription factor Stat5a and the nucleosome binding protein HMGN2, 4) engages with chromatin, and finally 4) aids in the activation of Stat5a-mediated gene expression. Collectively, our data imply that PRL-induced TAD phosphorylation initiates the co-activator activity of nuclear PRLr. Although potent TADs have been indentified in other transmembrane receptors (13, 39), this is the first study to identify that ligand-induced phosphorylation may be a key regulatory switch that triggers the transactivating function of a cell surface receptor.

We have performed numerous homology searches that have demonstrated the identified PRLr TAD is not shared by the larger family of cytokine receptor family members, however, this was not unexpected. First, this novel domain lies outside of the membrane-proximal Box 1, X box, Box 2, V box motifs shared amongst all cytokine receptor family members (40). Second, a report focusing on GHr, the cytokine receptor most similar to the PRLr (41) identified a TAD within the GHr ECD, rather than the ICD (39). Thus, it is possible that other cytokine receptor family members possess unique TADs in regions unique to that specific receptor.

There are now several reports suggesting how transmembrane receptors localize to the nucleus. One report suggests that the protein translocon Sec61 could extract a transmembrane protein from the lipid bilayer, expelling it into the cytoplasm and leaving it accessible for nuclear import (42). Another possible mechanism is one in which a protein within the nuclear import machinery assists in extricating a receptor from the plasma membrane. This has been observed for both FGFr and the GHr ECD, where the subsequent nuclear localization of these proteins seems to be dependent on importin α/β, a component of multiple nuclear import pathways (18, 22).

The PRLr TAD is rapidly phosphorylated in response to ligand **(Figure 4D)**. We propose that Jak2, which is bound to the PRLr and required for PRLr signal transduction, (8) may be the tyrosine kinase that is responsible for this rapid phosphorylation event. Jak2 has also been found in the nucleus, where in response to PRL, it phosphorylates the transcription factor NF1-C2 (43). However, since Jak2 activation alone is not sufficient for the full signaling properties of PRLr (44) it is possible that another kinase such as Src or Tec may be involved (45). We view these alternative kinases as less likely candidates since their kinetics of activation lag behind that of PRLr Y406 phosphorylation.

There are many lines of evidence that the nuclear localization of cell surface receptors may contribute to the pathology of malignant progression (12, 18, 46). In the context of these studies, we have seen that *in vitro*

overexpression of transactivation-deficient PRLrYDmut diminishes the ability of cells to grow in soft agar. *In vivo*, we have observed abundant PRLr Y406 phosphorylation in malignant breast tissue as compared to normal breast epithelium with particular nuclear enhancement in metastatic tissue (Fiorillo and Clevenger 2011, unpublished data). Collectively, these data point to a mechanism whereby the transactivating properties of cell surface receptors may correlate with a malignant state.

We have demonstrated that the PRLr TAD serves to recruit HMGN2, which in turn enhances the binding of PRLr and Stat5a to the *CISH* promoter. We hypothesize that in the larger PRLr/Stat5a/HMGN2 macromolecular complex, the following events occur: 1) Stat5a, provides the DNA binding domain that enables PRLr assembly onto chromatin, 2) the PRLr, through its TAD, tethers HMGN2 to the *CISH* promoter thereby providing DNA sequence specificity for HMGN2, and 3) HMGN2, by modulating nucleosome phasing or post-translational histone modifications, creates a more "open" chromatin conformation and enables the engagement of transcriptional elements that elevate levels of gene expression. A similar mechanism has been shown for the HMGN family member, HMGN3 (47). Here, siRNA-mediated depletion of HMGN3 prevented the binding of the transcription factor PDX1 to the *Glu2* promoter and in the absence of PDX1, HMGN3 could not bind *Glu2* (47). Given that HMGN family members do not possess DNA-sequence specificity, it is reasonable that an adapter molecule may be required for the binding of HMGN2 at specific loci. Therefore, HMGN2 and PRLr may depend on each other to mutually reinforce their chromatin binding stability and assembly onto chromatin. We propose that this may be one crucial step in a series of coordinated events that regulate *CISH* transcription.

There are numerous and sometimes contradictory studies describing the role of HMGN2 in transcription. Evidence has suggested that HMGN2 enables chromatin modifications, specifically H3K14 acetylation (Herrera et al., 1999). Using the murine orthologue of *CISH*, termed *Cis*, it has been demonstrated that in response to IL-3, H3K14 acetylation at the proximal promoter is modestly increased (48). However, this event was not sufficient for transcriptional activation implying that *Cis* chromatin remodeling may also depend on a factor involved in nucleosome sliding/displacement. Since the chromatin unfolding domain (CHUD) of HMGN proteins interacts with core histone tails and induces their rearrangement leading to chromatin decompaction, (49) HMGN2 could conceivably be the "missing link" involved in *Cis* transcriptional activation. Through its interaction with core histone tails, the CHUD may also serve to recruit factors that lead to post-translational histone modifications such as H3K14 acetylation. In preliminary studies, we have observed a reduction in H3K14 acetylation at the *CISH* promoter as a result of HMGN2 depletion, suggesting that this may be one mechanism by which HMGN2 activates *CISH* transcription (data not shown).

Several lines of evidence also support a second model for HMGN whereby it counteracts chromatin compaction by linker histones. This has been shown by footprinting of HMGN bound to nucleosome core particles which indicated that HMGN binding sites overlap with the proposed binding sites for the linker histones, namely histone H1 (50). These models (i.e. HMGN2-mediated chromatin modifications or HMGN2-mediated chromatin decompaction by linked histone competition) are not mutually exclusive and it is conceivable that HMGN could modulate the activity both of the linker histones and core histone tails within the same chromatin regions, or that one mechanism would take preference over another depending on the chromatin environment.

A larger question regarding transmembrane nuclear localization relates to the physiological context of receptors functioning both at the cell surface and in the nucleus. While it is recognized that surface receptors share many, if not most, of the same proximal signaling pathways, currently no model clearly describes how the cell distinguishes between different receptors that activate the same signaling cascades. The nuclear localization of transmembrane receptors could therefore provide a partial resolution to this conundrum of receptor/signaling pathway differentiation by contributing to specificity in output gene expression which would otherwise be compromised by the degeneracy of pathways shared among numerous receptors. We therefore propose that the ability of a cell surface receptor to recruit regulatory factors to specific promoter regions represents a general mechanism that may be applicable to the larger field of nuclear-localized cell surface receptors. In corroboration of our hypothesis and working model, two recent papers have been published, demonstrating interactions between EGFr/RNA Helicase (RHA) (51), and ErbB2/progesterone receptor (52), respectively. Additionally, it has been shown that the transcription factor, Coactivator Activator, can interact with a TAD within the GHr extracellular domain (39).

The concept of a nuclear transmembrane receptor functioning at both the non-genomic and genomic level can be paralleled to that of the estrogen receptor (ER). ERs have now been shown to function both as classic transcription factors and as signaling factors in the cytoplasm (53). This convergence of these ER functions at multiple response elements provides an exceedingly fine degree of control for regulating gene expression. Similarly, the convergence of the cell surface and genomic actions of the PRLr may provide a unique way for confer receptor/pathway specificity at the genomic level in order to finely tune target-gene expression.

As shown in **Figure 8**, we propose a working model in which: **1)** PRL stimulation induces PRLr TAD phosphorylation and PRLr nuclear localization, **2)** the PRLr-mediated recruitment of HMGN2 facilitates the association of PRLr and Stat5a with the *CISH* proximal promoter where Stat5a provides the DNA binding domain necessary for PRLr

chromatin occupancy, **3)** the coordinated assembly of HMGN2/ Stat5a/ PRLr onto chromatin initiates *CISH* transcriptional activation. We propose that this mechanism enables the cell to differentiate between multiple receptors that activate converging pathways by providing a direct connection between cell surface signaling and gene regulation in the nucleus. Given that an activated PRLr TAD is required for anchorage-independent growth and the phosphorylation of PRLr-Y406 is present in malignant breast tissue, the observations presented here may have direct pathophysiologic relevance.

8.1.5 Materials and Methods

Prolactin treatment

Human recombinant PRL was a gift from Dr. Anthony Kossiakoff, University of Chicago. PRL was added to cells to yield a final concentration of 250 ng/mL.

Cell lines and culture

T47D and MCF7 human breast cancer cell lines were obtained from American Type Culture Collection (Manassas, VA) and cultured in DMEM (Dulbecco's Modified Eagle Medium) supplemented with 10% FBS (fetal calf serum), 100 units/mL penicillin, and 100 μg/mL streptomycin (Gibco, Grand Island, NY). 293T/17 cells with stable integration of the SV40 large T antigen and HLR cells with stable integration of the Gal4-UAS luciferase reporter were supplied by Dr. Debu Chakravarti and were cultured in DMEM with 10% FBS and 100ug/mL streptomycin. MCF10Adelp53 cell lines were a gift from Dr. Serge Fuchs and were cultured in DMEM/F-12 media supplemented with 10% FBS, 100 units/mL pen/strep. All cells were incubated in a humidified 5% CO_2/95% air atmosphere at 37°C.

Plasmids

Wild type PRLr in pTracer and the *CISH*-luciferase reporter constructs have been previously described (10). PRLr cDNAs, NLS-ICD and PRL-NLS were created using PCR which additionally added the SV-40 nuclear localization signal (GCCCTAAAAAGAAGCGTAAAGTCG) to each product. PCR products were ligated into pTracer EF-V5/His (Invitrogen) using EcoRI and NotI restriction sites. Gal4-PRLr constructs were generated by PCR to amplify specific regions of the PRLr intracellular or extracellular domains. PRLr cDNAs were then cloned into Gal4-pCMX vector using EcoRI and EcoRV restriction sites. PRLrYDmut was generated using QuikChange Lightning mutagenesis (Stratagene) using the parental PRLr pTracer construct.

pCMV-XL5 containing HMGN2 cDNA was purchased (Origene). NBDmut was constructed using QuikChange lightning site-directed mutagenesis. All mutagenesis primer sequences are listed in **Table SI**.

Cell Fractionation

T47D cells were grown in 150 mm dishes until they reached 70% confluency. MCF7 or CHO cells were plated 24 h. prior to transfection in 100mm dishes, then transfected with 2ug of PRLr cDNA using Fugene HD (Roche). Cytoplasmic

and nuclear extracts were subsequently obtained using NE-PER (Pierce) according to the manufacturer's protocol. 5X laemmli buffer was added to non-nuclear and nuclear samples. Samples were then boiled for 5 min, then subjected to SDS-Page using a 4-20% Tris-HCl gradient gel (Bio-Rad). Proteins were then transferred to a polyvinylidene difluoride filters (PVDF). The filters were blocked in casein blocker (Pierce) for 1 h. Following blocking, the blots were incubated with the one of the following primary antibodies overnight at 4^0C: anti-PRLr ECD (Invitrogen), anti-PRLr-ICD (Santa Cruz), anti-Histone H3 (Abcam), anti-Lamin B1 (abcam), anti-Calnexin (BD Biosciences). Antibodies were diluted in casein blocker/TBS + 0.05% tween). Filters were washed three times with TBS + 0.05% tween, then probed with horseradish peroxidase–conjugated secondary antibody for 1 hour at room temperature. Chemiluminescence was detected with ECL Plus (Amersham), and images were collected on a charge-coupled device camera (Fuji).

Immuohistochemistry

Immunohistochemical analysis, as previously described (4), was carried out with an anti-PRLr antibody (Santa Cruz). Sections of 5µm from formalin-fixed paraffin-embedded tissue microarrays were deparaffinized in xylene and rehydrated in graded alcohol. After deparaffinization, heat induced antigen retrieval by boiling slides in 10 mM citrate buffer pH 6.0 for 20 min was carried out. The sections were blocked with a peroxidase blocking system (Dako, Carpinteria CA, USA) for 10 min. Sequential incubations included the following: 2% normal goat serum for 20 min; anti-PRLr antibody at 1:25 dilution for 60 min at RT; secondary biotinylated anti-rabbit IgG for 30 min; and, finally, the streptavidin-biotinylated horseradish peroxidase complex reagent (Dako) for 30 min at RT. After incubations slides were washed three times in buffer for 3 min each. Sections were then exposed to the chromagen DABplus (Dako) for 5 min and were counterstained in hematoxylin, dehydrated, cleared and mounted. In this analysis the nuclear intensity of tissue samples was scored from 0 to 3, and a score above 1.5 was counted as positive, as previously described (4).

Biotinylation

Biotinylation was performed using sulfo-NHS biotin (Pierce) according to manufacturer's protocol. T47D cells in were grown in 150 mm dishes to 70% confluency, then serum starved for 24 h. prior to biotinylation. Cells were lifted off dishes with versene, washed three times with 10 ml of PBS and resuspended in 200ul of 2mM sulfo-NHS-biotin (Pierce) for 30 min at 4^oC (to prevent active internalization). Reactions were quenched for 10 min with 500uL PBS containing 100 mm glycine. Cells were stimulated with PRL for 0, 10 and 30 min. at 37^oC. Samples were then separated into non-

nuclear and nuclear fractions using NE-PER (Pierce) according to manufacturer's protocol, 10% of each sample was aliquoted for input. Nuclear lysates were diluted with dilution buffer (20% Glycerol, 1% triton X-100). Streptavidin-agarose beads (Pierce, 50 µl of a 50:50 slurry) were then added to 500 µl nuclear and nuclear fractions, and the suspension was rocked overnight at 4 °C. The beads were washed five times with respective lysis buffers (CER or NER). Proteins were then eluted from beads using 2X lammeli buffer and boiled for 5 min then resolved by SDS-Page on a 4-20% gradient gel (Bio-Rad) and transferred to a PVDF membrane. Membranes were blocked as stated above (see cell fractionation), probed with the following primary antibodies overnight at 4^{o}C: anti-PRLr-ICD antibody and anti-β1 integrin antibody (Abcam) as a negative control. Membranes were then developled as stated above (see cell fractionation). 5x lamelli buffer was added to input samples, then samples were treated as above. Membranes with input proteins were probed with an anti-calnexin primary antibody to control for non-nuclear contamination in nuclear samples.

Luciferase assay

Luciferase assays that utilized the *CISH*-luciferase reporter were conducted as previously described using MCF7 cells (10). Luciferase assays using the Gal4-UAS reporter construct were conducted as follows. 293T cells were seeded into a 24 well plate at a density of 1.5x10^{5}. Cells were transfected with 250 ng of luciferase reporter, 2ng of renilla reporter, and 10 ng of Gal4-PRLr constructs using lipofectamine 2000. Twenty-four hours post-transfection were lysed through luciferase assay using Dual Reporter Luciferase reagents (Promega) and read by a Victor Microplate Reader (Perkin Elmer). All transfections were performed in triplicate or quadruplicate, and each individual sample was read in duplicate. The ratio of luciferase/renilla was calculated and the results are reported as fold change compared to an empty vector control (Gal4-UAS reporter) or an untreated empty vector control (*CISH* reporter, LHRE reporter.)

Cell Fractionation and Nuclear Co-Immunoprecipitation

Cells were grown in 150 mm dishes until they reached 70% confluency, followed by arrest for 24 h. Cells were then treated with PRL (250 ng/ml) for the indicated times (0, 10 or 30 min.). Cytoplasmic and nuclear extracts were subsequently obtained using NE-PER (Pierce) according to the manufacturer's protocol. Nuclear lysates were diluted with dilution buffer (20% Glycerol, 1% triton X-100). 4 µg of anti-Stat5a (Invitrogen) or anti-PRLr (Santa Cruz) antibodies were added and samples were rocked overnight at 4^{o}C. Subsequently, 50 µl of Dynal protein G magnetic beads (Invitrogen) were added for 1 h and samples were collected on a magnetic particle concentrator (DynaMag-2, Invitrogen)

and washed in the appropriate buffer; cytosolic samples were washed in CER lysis buffer, and nuclear samples were washed in dilution buffer. Bound proteins were recovered in 2X laemmli buffer and subjected to SDS-Page using a 4-20% Tris-HCl gradient gel (Bio-Rad). Proteins were then transferred to a PVDF membrane and normal immunoblot procedures were followed as stated above.

Chromatin Immunoprecipitation

Chromatin immunoprecipitation was conducted as previously described (54) until DNA isolation, then the Fast ChIP was employed (55). Specifically, T47D cells were arrested in phenol-free medium for 24 h before PRL treatment (250ng/ml) for 30 min. Anti-PRLr, anti-Stat5 (Santa Cruz) anti- HMGN2 (Millipore) and anti-H3K14 (Millipore) antibodies were used to immunoprecipitate protein-DNA complexes. Eluted DNA was subjected to real-time PCR analysis and was normalized to input. The fold change was subsequently normalized to an IgG or beads only control. Primers for specific amplicons are listed in **Table SII.**

Retroviral production

Overexpression cell lines: PRLr or PRLr YDmut in pTracer were amplified through PCR and ligated into the retroviral pBabe-GFP vector using EcoRI and SalI. Knockdown cell lines: a pre-designed HMGN2 shRNA pRFP retroviral vector was purchased from Origene and the PRLr shRNA was designed and cloned into pRFP vector (Sequences HMGN2: GTGTCAGGCAATCTGGACTTTCCAGTGAT; PRLr CAACTGCATAACCTTTACACT). Recombinant retroviruses for pBabe, PRLr, PRLrYDmut, Scrambled shRNA, shHMGN2 and shPRLr were generated using transfection of retroviral vectors with Lipofectamine 2000 (Invitrogen) in 293T/17 cells along with pVSVG and pGalPol vectors. Viral supernatant was collected 48 hours post-transfection and added to the appropriate cell lines along with 8 µg/mL polybrene. Cells were spin-infected at 500g for 2 hours at 32^{o}C. Infected cells were enriched by FACS sorting for GFP (overexpression cell lines) or puromycin selection (knockdown cell lines).

HMGN2 Co-Immunoprecipitation

Stably transfected T47D cells (expressing Empty vector, wt PRLr or PRLrYDmut) or stably transfected MCF7 cells expressing Empty vector, wt PRLr or PRLrYDmut) were grown in 150 mm dishes until 70% confluency followed by

arrest for 24 h. before PRL treatment. Cells were washed with PBS and then pelleted at 1000g and 10% of each sample was taken for input. Cell lysis and immunoprecipitation was then conducted as previously described (56). Samples were subjected to co-immunoprecipitation with 4 µg of either an anti-HMNG2 antibody (Millipore) an anti-V5 antibody (Invitrogen) to recognize PRLr or an anti-Gal4 antibody (Santa Cruz) to recognize PRLr truncation constructs. Antibodies were added to samples and incubated overnight at 4°C. 50 µl of Dynal protein G magnetic beads (Invitrogen) were added for 1 h and samples were collected on a magnetic particle concentrator (DynaMag-2, Invitrogen) and washed in the appropriate buffer (see Zhu and Hansen). Bound proteins were recovered in 2x Laemmli buffer and run on a 4-20% Tris-HCl gradient gel (Bio-Rad), followed by western blot analysis. Membrane was blocked with casein blocker (Pierce), probed with anti-V5 or anti-HMNG2 antibodies and visualized by chemiluminesence (GE Healthcare).

RT-PCR and real-time PCR

Total RNA was isolated from the following cells: MCF7 and MCF10AΔp53 stable cells expressing PRLr constructs, MCF7 cells with transient transfection of HMGN2 contructs, T47D cells with transient or stable knockdown of HMGN2. RNA was isolated using EZ mini-prep kit (Qiagen) as previously reported (57). cDNA was synthesized using qScript (Quanta Biosciences). cDNA was diluted to 2.5 ng/µl (corresponding to RNA concentration). 4 µl cDNA, 1 µl primers (2 µM each), and 5 µl 2x Power SYBR MasterMix was used for real-time PCR in 10 µl reaction volume performed in a 384-well plate. Real-time PCR was conducted on an ABI 7900HT thermocycler (Applied Biosystems, Foster City, CA). All real-time PCR were run in triplicate. For RT-PCR, data were normalized to GAPDH RNA or 18S rRNA. Fold change for RT-PCR is represented as $2^{-\Delta\Delta Ct}$($2^{-(Cttarget-Ct18SrRNA)PRL-(Cttarget-Ct18SrRNA)control}$) using Empty vector, non-treated as a baseline. Primers used are listed in **Table SII**.

Immunofluoresence

T47D cells were grown on four-well chamber slides to ~50% confluency in normal growth media before staining with anti-phospho PRLrY406 (NEB). Cells were arrested for 24 h. then treated with PRL for 0, 5 and 15 min. Cells were rinsed in PBS and then fixed in 4% paraformaldehyde/0.1M phosphate buffer (pH 7.4) for 10 min. Cells were blocked with blocking solution (PBS, 1%BSA, 0.05% Triton X-100) for 15 minutes at room temperature and then incubated with a 1:25 dilution of anti-phospho Y406 PRLr (NEB) diluted in blocking solution for 2 hours at RT. After washing with wash solution (PBS, 0.05% Triton X 100) cells were incubated with a 1:800 dilution of secondary antibody conjugated to

Alexafluor-388 (Invitrogen) for 30 min. Cells were washed twice with PBS, and stained with Hoechst (1ug/mL in PBS) for 3 min. Cells were washed three times with PBS, and then mounted using anti-fade mounting medium (Vector Laboratories Inc.). Images were visualized using confocal microscopy.

Western Blotting

For signaling studies, the indicated cell lines (PRLr-expressing T47D, PRL-expressing MCF10AΔp53 and CHO cells transiently transfected with wtPRLr or PRLrYDmut) were plated in 10mm dishes at 70% confluency. Cells were arrested and treated with 250 ng/mL PRL for the indicated time courses. Cells were lysed in RIPA buffer and subjected to western blot as described above. Blots were probed with anti-Akt (Cell Signaling), anti-phospho-Akt (Cell signaling), anti-Erk, (Cell-signaling), anti-phospho Erk (Cell Signaling), anti-Stat5a (Santa Cruz) and anti-phospho Stat5a antibodies (Invitrogen).

siRNA-mediated knockdown

siRNA knockdown experiments were conducted in T47D cells as has been previously reported (58). The Accell SMART pool siRNAs against HMGN1 were purchased from Thermo Scientific catalogue number E-015567-00-0005. The siRNA against HMGN2 was purchased through Origene catalogue number SR302144, sequence #3.

Soft agar

Soft Agar was carried out as previously described (59). Colony size and number were quantified using ImageJ software (NIH).

Statistical Analysis

Statistical analysis was performed using one-way or two-way ANOVA on GraphPad Prism 4 (La Jolla, CA). The results are shown as the means with error bars depicting ± SEM. $P < 0.05$ is considered as statistically significant with * $p<0.05$, ** $p<0.01$, *** $p<0.001$. All experiments were performed at least three times unless otherwise indicated.

8.1.6 Figure Legends

Figure 1. The PRLr is present in the nucleus and is translocated from the cell surface. (A-B) Cell fractionation and western blot analysis. T47D cells in normal growth conditions were partitioned into nuclear and non-nuclear fractions. An anti-PRLr antibody specific to the extracellular domain **(A)** or intracellular domain **(B)** were used to demonstrate the nuclear presence of full-length PRLr. To demonstrate that proteins from the endoplasmic reticulum (ER) are not contaminating nuclear fractions non-nuclear fractions were also probed with anti-calnexin, an integral ER membrane protein. Similarly, nuclear fractions were probed with anti-histone H3 or anti-Lamin B1 antibodies to demonstrate nuclear purity. Whole cell lysate samples are shown parallel to nuclear and non-nuclear fractions. **(C)** Immunohistochemical analysis of nuclear PRLr in normal, DCIS and invasive breast tissue. Tissues were stained with an anti-PRLr ICD antibody. **(D)** Biotinylation assay to detect cell-surface PRLr in the nucleus of PRL-stimulated T47D cells. T47D cells were serum starved for 24 h. before biotinylation and PRL treatment. After cell fractionation nuclear and non-nuclear fractions were immunoprecipitated with streptavidin beads. Eluted proteins were analysis by western blot analysis, and probed with anti-PRLr. 10% of nuclear and non-nuclear lysates were taken out prior to immunoprecipitation and analyzed by western analysis for ER contamination in the nucleus using an anti-calnexin antibody. In a parallel experiment, T47D cells were biotinylated and PRL-treated. After streptavidin immunoprecipitation, samples were analyzed by western blot using an anti-β1 integrin antibody to demonstrate a biotinylated cell surface protein that is internalized, but does not localize to the cell nucleus.

Figure 2. Nuclear PRLr associates with Stat5a and facilitates Stat5a-driven gene expression. (A) T47D cells were serum starved for 24h. prior to PRL treatment (10 min). Cells were then partitioned into non-nuclear and nuclear lysates and subjected to Co-immunoprecipitation analysis using an anti-Stat5a antibody. Eluted samples were analyzed by western blot analysis using an anti-PRLr antibody. Blots were stripped and re-probed for anti-Stat5a. 10% of non-nuclear and nuclear lysates were aliquoted prior to immunoprecipitation and analyzed by western analysis using an anti-calnexin antibody as a control for contamination in the nucleus. **(B)** Top; Detail of the *CISH* promoter; arrows delineate primers used for chromatin immunoprecipitation (ChIP). The primer sets represent the following amplicons;
(-104/-68), the *CISH* proximal promoter and (+311/+380), the CISH downstream coding region. *Bottom***;** PRLr association at the indicated regions as assayed by chromatin immunoprecipitation. PRLr occupancy at the *CISH* proximal promoter or a downstream coding region was analyzed using a PRLr-ECD antibody. IgG demonstrates the negative

control in this experiment and all results are reported as fold change by normalizing to IgG conditions. The values are those of a representative experiment repeated three separate times, where SEM indicates the error of three replicate measurements within one experiment. **(C)** *Top;* Schematic of constructs to force the nuclear localization of PRLr by the addition of an SV40 NLS. Constructs as termed PRLr-NLS or NLS-ICD. *Bottom*; Schematic of *CISH* luciferase reporter. **(D)** *CISH* luciferase activity in MCF7 cells transfected with the indicated cDNAs. Cells were transfected with cDNAs for 24 h, serum starved for 24h. then treated with PRL for an additional 24 h. Results are presented as fold change relative to non-treated empty vector control. Values are those of a representative experiment repeated three separate times where SEM represents the error of three replicates performed within one experiment.

Figure 3. Identification of a novel PRLr TAD. (A) *Top;* Schematic of Gal4-UAS luciferase reporter and Gal4-DBD PRLr fusion construct. UAS = upstream activating sequence, DBD = DNA binding domain. *Bottom*; Schematic of Gal4-ECD, Gal4-ICD, Gal4-Stat5aTAD, or Gal4 control constructs. **(B)** Gal4-UAS luciferase activity in 293T cells transfected with Gal4-ECD, Gal4-ICD, Gal4-Stat5aTAD, or Gal4 control constructs. **(C)** Gal4-UAS luciferase assay measuring transactivation of PRLr C-terminal truncation constructs in 293T cells. **(D)** Gal4-UAS luciferase activity of Gal4 fusion constructs in 293T cells with the indicated PRLr regions as determined by **C**. **(E)** Cross-species sequence alignment of the identified PRLr TAD highlighting four conserved residues (gray). **(F)** Gal4-UAS luciferase activity of the TAD point mutations in 293T cells as determined in **F**. Reported values are those of a representative experiment repeated three separate times, where SEM indicates the error of quadruplicate transfections performed within one experiment.

Figure 4. The PRLr transactivation domain contributes to Stat5a-mediated gene expression. (A) Real time PCR performed on cDNA collected from PRL-treated MCF7 stable cell pools **(B)** to determine *CISH* mRNA induction. MCF7 transfectants were serum starved for 24 h. prior to 2h. PRL treatment. Values were normalized to GAPDH RNA and fold change was calculated by comparing each value to the non-treated control sample and are representative of three separate experiments with SEM. **(B)** Western blot analysis of CHO cells transiently transfected with Stat5a, Jak2, and either empty vector, PRLr, or PRLrYDmut constructs. Cells were transfected, and then serum starved for 24 h. prior to PRL treatment (15 min). Blots were probed with antibodies against phosphStat5a or Stat5a and demonstrate the ability of PRLrYDmut to activate Stat5a. **(C)** Co-immunoprecipitation assays performed in PRL-treated T47D stable cells expressing PRLrYDmut. PRL- treated non-nuclear and nuclear lysates were subjected to co-immunoprecipitation using

an anti-V5 antibody to precipitate PRLrYDmut. Bound proteins were analyzed by western blot using an anti-Stat5a antibody. Blots were stripped and re-probed using an anti-V5 antibody to demonstrate proper pull down of mutant PRLr **(D)** PRL-treated T47D cell lysates subjected to Co-IP using an anti-PRLr antibody. Precipitates were analyzed by western blot with an anti-phosphoY406 PRLr antibody and demonstrate the phosphorylated of PRLr Y406 in a ligand-inducible manner. **E)** Immunofluoresence images in T47D cells using confocal microscopy. T47D cells were plated in chamber well slides and grown to 30% confluency then serum starved for 24h. Cells were treated with PRL for 0, 5 or 15 min, then fixed and stained with an anti-phospho Y406 PRLr antibody. *Green=PRLr phosphoY406 PRLr and red=DAPI stained nuclei*. **(F)** Co-immunoprecipitation analysis of PRL-treated MCF7 stable cell pools expressing wild-type PRLr or PRLrYDmut. Bound proteins were analyzed by western analysis using an anti-phosphoY406 PRLr antibody.

Figure 5. HMGN2 mediates PRLr transactivation activity. (A) Co-immunoprecipitation performed on HLR cells (with stable integration of Gal4-UAS) with transient transfection of the indicated Gal4 constructs. Anti-Gal4 precipitates were subjected to western blot analysis with an anti-HMGN2 antibody. **(B)** HMGN2 co-immunoprecipitation in PRL-treated (30 min) T47D cells expressing V5-tagged PRLr and PRLrYDmut. Western blots were analyzed with anti-V5 (PRLr), anti-HMGN2 or anti-phospho PRLr Y406 antibodies. **(C)** ChIP analysis performed on PRL-treated T47D cells using an anti-HMGN2 antibody. Standard conditions (24h. serum starvation, 30 min PRL treatment) were used. **(D)** *CISH* luciferase activity in MCF7 cells transfected with the indicated constructs. MCF7 cells were serum starved for 24 h. then treated for 24 h. with PRL. Results are representative of 3 separate experiments with SEM. **(E)** Real time PCR performed on cDNA collected from T47D cells with stable expression of non-specific shRNA (shNS) or shRNA against HMGN2 (shHMGN2). Stable T47D cells were serum starved for 24 h. prior to 0, 1 or 4 h. PRL treatment. **(F)** Real time PCR performed on cDNA collected from MCF7 transfected with HMGN2 or NBDmut cDNA expression vectors. MCF7 cells were plated 24h. post transfection. 2 μg HMGN2 or NBDmut cDNA were then transfected into cells using Fugene HD. 24 h. post-transfection cells were serum starved for an additional 24h. Cells were then treated with PRL for 1h. The values are those of a representative experiment repeated three separate times, where SEM indicates the error of three replicate measurements within one experiment.

Figure 6. HMGN2 knockdown impairs PRLr and Stat5a promoter binding. (A-B) shNS or shHMGN2 cells were serum starved for 24 h. prior to PRL treatment. Cells were then subjected to chromatin immunoprecipitation using anti-

PRLr **(A)** or anti-Stat5a **(B)** antibodies. IgG demonstrates the negative control in this experiment and all results are reported as fold change by normalizing to IgG conditions. The values are those of a representative experiment repeated two separate times, where SEM indicates the error of three replicate measurements within one single experiment.

Figure 7. The PRLr TAD promotes a transformed phenotype. (A) MCF10AΔp53 c transfectants were suspended in a 0.3% agar-medium mix supplemented with PRL (250 ng/mL) for 10 days. ach condition was photographed under phase-contrast optics. **(B)** Quantification of the average colonies per field. Each condition was set up in triplicate wells and error bars represent SEM.

Figure 8. Model for signal-dependent PRLr transactivation.

1) Ligand induces PRLr Y406 phosphorylation and PRLr nuclear localization. **2)** PRLr-mediated recruitment of HMGN2 facilitates engagement of the PRLr/Stat5a/HMGN2 complex onto the *CISH* promoter. **3)** The coordinated assembly of this complex promotes *CISH* transcriptional activation.

8.1.7 Supplemental Information

Supplemental Figure Legends

Figure S1. The PRLr localizes to the nucleus. (A-B) Cell fractionation and western blot analysis in cells transiently transfection with PRLr cDNA. MCF7 **(A)** or CHO **(B)** cells were transfected with a V5-tagged PRLr cDNA construct. 48 h. post-transfection cells in normal growth conditions were partitioned into nuclear and non-nuclear fractions. An anti-V5 antibody specific (to recognize PRLr) was used to demonstrate the nuclear presence of full-length PRLr.. To demonstrate that proteins from the endoplasmic reticulum (ER) are not contaminating nuclear fractions non-nuclear fractions were also probed with anti-calnexin, an integral ER membrane protein or anti-KDEL, a receptor in the ER that functions in protein folding and assembly . **(C)** No-antibody negative control for immunohistochemical analysis in Figure 1C.

Figure S2. Nuclear PRLr participates in Stat5a-mediated gene expression. (A) T47D cells were serum-starved for 24h. prior to treatment with PRL (30 min). Cells were then partitioned into non-nuclear and nuclear fractions and subjected to co-immunoprecipitaion analysis using an anti-PRLr ECD antibody. Results demonstrate the ligand-dependent association of PRLr and Stat5a in the nucleus. **(B)** T47D cells were serum-started for 24h. prior to 30 min treatment with PRL. Chromatin immunoprecipitation was then performed using an anti-Stat5a antibody to demonstrate Stat5a occupancy at the *CISH* proximal promoter upon PRL stimulation. **(C)** ChIP assay as performed in B, using an anti-PRLr ICD antibody to demonstrate PRLr occupancy at the *CISH* proximal promoter upon PRL (30 min) stimulation. Reported values are those of a representative experiment repeated three separate times, where SEM indicates the three replicates within one experiment. **(D)** Western blot to assay expression of wild-type PRLr, PRLr-NLS or NLS-ICD in 293T cells. **(E)** Luciferase assay measuring the activity of the *CISH* reporter in MDA-231 cells expressing the indicated constructs, as performed in 2E. Reported values are those of a representative experiment repeated three separate times, where SEM indicates the error of triplicate transfections performed within one experiment.

Figure S3. The PRLr transactivation domain is necessary for Stat5a-mediated gene expression. (A-B) Western analysis of MCF10AΔp53 **(A)** or MCF7 **(B)** stable cell pools expressing V5 tagged PRLr, PRLrYDmut or empty vector control. **(C)** Real time PCR performed on cDNA collected from PRL-treated MCF10AΔp53 stable cell pools to determine CISH mRNA induction. Values were normalized to GAPDH RNA and fold change was calculated by comparing each value to the non-treated control sample and are representative of three separate experiments where SEM demonstrates the error between replicates within one experiment. **(D)** *CISH* luciferase activity in MCF7 cells transfected with PRLr, PRLrYDmut, or an empty vector control. **(E)** Western analysis of MCF10AΔp53 stable cell pools using phospho-specific antibodies against Erk and Akt.

Figure S4. HMGN2 depletion impairs CISH mRNA induction while HMGN1 depletion has no effect. (A) HMGN2 shRNA knockdown efficiency measured by RT-PCR. **(B)** Western blot analysis of T47D stable knockdown cell pools expressing shRNA against HMGN2 or a control sequence, termed shHMGN2 or shNS. **(C)** HMGN2 siRNA knockdown efficiency measured by RT-PCR. **(D)** Real time RT-PCR performed on T47D cells transfected with control or HMGN2 siRNA. **(E)** HMGN1 knockdown efficiency measured by RT-PCR. **(F)** Real time RT-PCR was performed on T47D cells transfected with HMGN1 siRNA or a control siRNA and treated with PRLr for 1 or 4 h. in order to assess *CISH* transcript levels. Reported values are those of a representative experiment repeated three separate times, where SEM indicates the error of quadruplicate transfections performed within one experiment.

Supplemental Tables

Table SI. Primer sets for site-directed mutagenesis

Construct	Primer set
PRLrYDmut	olg388GCCAGCACAACCCCAGATCCTCTTTCCACAATATTACTGCCGTGTGTGAGC olg389GCTCACACACGGCAGTAATATTGTGGAAAGAGGATCTGGGGTTGTGCTGGC
NBDmut	olg 409 CACAGAGAAGAGAGGCGAGGTTGGAGGCTAAACCTGC olg410 GCAGGTTTAGCCTCCAACCTCGCCTCTCTTCTCTGTG

Table SII. Primers for RT-PCR and ChIP

Gene name	primer sequences (5'-3')	Amplicon
RT-PCR		
GAPDH	olg74CATGAGAAGTATGACAACAGCCT olg75 AGTCCTTCCACGATACCAAAGT	511-623
CISH	olg133 AGAGGAGGATCTGCTGTGCAT olg134 GGAACCCCAATACCAGCCAG	311-380
PRLr	olg151 CACAACCCCAGATCCTC olg152 GGCGTATCCTGGTCAGTCTC	1267-1472
HMGN1	olg407 CGCGGTTGTCAGCTAAACCT olg408 TCGCTGCTGCCTTTTTCG	65-124
HMGN2	olg392 GCAAAGGTGAAGGACGAAC olg 393 GTACCTTCTCTCCCTTCTTTG	43-157
ChIP		
CISH proximal promoter	olg108 AGCCCGCGGTTCTAGGAA olg109 AGCTGCTGCCTAATCCTTTGTC	-140/ -68
CISH coding	olg133 AGAGGAGGATCTGCTGTGCAT olg134 GGAACCCCAATACCAGCCAG	+311/+380

8.1.8 References

1. Reynolds C, Montone KT, Powell CM, Tomaszewski JE, Clevenger CV 1997 Expression of prolactin and its receptor in human breast carcinoma. Endocrinology 138:5555-5560
2. Yamashita H, Nevalainen MT, Xu J, LeBaron MJ, Wagner KU, Erwin RA, Harmon JM, Hennighausen L, Kirken RA, Rui H 2001 Role of serine phosphorylation of Stat5a in prolactin-stimulated beta-casein gene expression. Mol Cell Endocrinol 183:151-163
3. Harris J, Stanford PM, Sutherland K, Oakes SR, Naylor MJ, Robertson FG, Blazek KD, Kazlauskas M, Hilton HN, Wittlin S, Alexander WS, Lindeman GJ, Visvader JE, Ormandy CJ 2006 Socs2 and elf5 mediate prolactin-induced mammary gland development. Mol Endocrinol 20:1177-1187
4. McHale K, Tomaszewski JE, Puthiyaveettil R, Livolsi VA, Clevenger CV 2008 Altered expression of prolactin receptor-associated signaling proteins in human breast carcinoma. Mod Pathol 21:565-571
5. Li Y, Clevenger CV, Minkovsky N, Kumar KG, Raghunath PN, Tomaszewski JE, Spiegelman VS, Fuchs SY 2006 Stabilization of prolactin receptor in breast cancer cells. Oncogene 25:1896-1902
6. Hankinson SE, Willett WC, Michaud DS, Manson JE, Colditz GA, Longcope C, Rosner B, Speizer FE 1999 Plasma prolactin levels and subsequent risk of breast cancer in postmenopausal women. J Natl Cancer Inst 91:629-634
7. Rui H, Kirken RA, Farrar WL 1994 Activation of receptor-associated tyrosine kinase JAK2 by prolactin. J Biol Chem 269:5364-5368
8. Lebrun JJ, Ali S, Sofer L, Ullrich A, Kelly PA 1994 Prolactin-induced proliferation of Nb2 cells involves tyrosine phosphorylation of the prolactin receptor and its associated tyrosine kinase JAK2. J Biol Chem 269:14021-14026
9. Brockman JL, Schroeder MD, Schuler LA 2002 PRL activates the cyclin D1 promoter via the Jak2/Stat pathway. Mol Endocrinol 16:774-784
10. Fang F, Antico G, Zheng J, Clevenger CV 2008 Quantification of PRL/Stat5 signaling with a novel pGL4-CISH reporter. BMC Biotechnol 8:11
11. Raccurt M, Tam SP, Lau P, Mertani HC, Lambert A, Garcia-Caballero T, Li H, Brown RJ, McGuckin MA, Morel G, Waters MJ 2003 Suppressor of cytokine signalling gene expression is elevated in breast carcinoma. Br J Cancer 89:524-532
12. Lo HW, Xia W, Wei Y, Ali-Seyed M, Huang SF, Hung MC 2005 Novel prognostic value of nuclear epidermal growth factor receptor in breast cancer. Cancer Res 65:338-348
13. Lin SY, Makino K, Xia W, Matin A, Wen Y, Kwong KY, Bourguignon L, Hung MC 2001 Nuclear localization of EGF receptor and its potential new role as a transcription factor. Nat Cell Biol 3:802-808
14. Komuro A, Nagai M, Navin NE, Sudol M 2003 WW domain-containing protein YAP associates with ErbB-4 and acts as a co-transcriptional activator for the carboxyl-terminal fragment of ErbB-4 that translocates to the nucleus. J Biol Chem 278:33334-33341
15. Ni CY, Murphy MP, Golde TE, Carpenter G 2001 gamma -Secretase cleavage and nuclear localization of ErbB-4 receptor tyrosine kinase. Science 294:2179-2181
16. Offterdinger M, Schofer C, Weipoltshammer K, Grunt TW 2002 c-erbB-3: a nuclear protein in mammary epithelial cells. J Cell Biol 157:929-939
17. Lobie PE, Wood TJ, Chen CM, Waters MJ, Norstedt G 1994 Nuclear translocation and anchorage of the growth hormone receptor. J Biol Chem 269:31735-31746
18. Conway-Campbell BL, Wooh JW, Brooks AJ, Gordon D, Brown RJ, Lichanska AM, Chin HS, Barton CL, Boyle GM, Parsons PG, Jans DA, Waters MJ 2007 Nuclear targeting of the growth hormone receptor results in dysregulation of cell proliferation and tumorigenesis. Proc Natl Acad Sci U S A 104:13331-13336
19. Marti U, Wells A 2000 The nuclear accumulation of a variant epidermal growth factor receptor (EGFR) lacking the transmembrane domain requires coexpression of a full-length EGFR. Mol Cell Biol Res Commun 3:8-14
20. Feng S, Xu J, Wang F, Kan M, McKeehan WL 1996 Nuclear localization of a complex of fibroblast growth factor(FGF)-1 and an NH2-terminal fragment of FGF receptor isoforms R4 and R1alpha in human liver cells. Biochim Biophys Acta 1310:67-73
21. Johnston CL, Cox HC, Gomm JJ, Coombes RC 1995 Fibroblast growth factor receptors (FGFRs) localize in different cellular compartments. A splice variant of FGFR-3 localizes to the nucleus. J Biol Chem 270:30643-30650

22. Reilly JF, Maher PA 2001 Importin beta-mediated nuclear import of fibroblast growth factor receptor: role in cell proliferation. J Cell Biol 152:1307-1312
23. Hung LY, Tseng JT, Lee YC, Xia W, Wang YN, Wu ML, Chuang YH, Lai CH, Chang WC 2008 Nuclear epidermal growth factor receptor (EGFR) interacts with signal transducer and activator of transcription 5 (STAT5) in activating Aurora-A gene expression. Nucleic Acids Res 36:4337-4351
24. Lo HW, Hung MC 2006 Nuclear EGFR signalling network in cancers: linking EGFR pathway to cell cycle progression, nitric oxide pathway and patient survival. Br J Cancer 94:184-188
25. Lo HW, Cao X, Zhu H, Ali-Osman F 2010 Cyclooxygenase-2 is a novel transcriptional target of the nuclear EGFR-STAT3 and EGFRvIII-STAT3 signaling axes. Mol Cancer Res 8:232-245
26. Rao YP, Buckley DJ, Buckley AR 1995 The nuclear prolactin receptor: a 62-kDa chromatin-associated protein in rat Nb2 lymphoma cells. Arch Biochem Biophys 322:506-515
27. Rao YP, Buckley DJ, Olson MD, Buckley AR 1995 Nuclear translocation of prolactin: collaboration of tyrosine kinase and protein kinase C activation in rat Nb2 node lymphoma cells. J Cell Physiol 163:266-276
28. LeBaron MJ, Xie J, Rui H 2005 Evaluation of genome-wide chromatin library of Stat5 binding sites in human breast cancer. Mol Cancer 4:6
29. Litterst CM, Kliem S, Marilley D, Pfitzner E 2003 NCoA-1/SRC-1 is an essential coactivator of STAT5 that binds to the FDL motif in the alpha-helical region of the STAT5 transactivation domain. J Biol Chem 278:45340-45351
30. Li S, Shang Y 2007 Regulation of SRC family coactivators by post-translational modifications. Cell Signal 19:1101-1112
31. Naar AM, Lemon BD, Tjian R 2001 Transcriptional coactivator complexes. Annu Rev Biochem 70:475-501
32. Gadd SL, Clevenger CV 2006 Ligand-independent dimerization of the human prolactin receptor isoforms: functional implications. Mol Endocrinol 20:2734-2746
33. Crippa MP, Alfonso PJ, Bustin M 1992 Nucleosome core binding region of chromosomal protein HMG-17 acts as an independent functional domain. J Mol Biol 228:442-449
34. Postnikov YV, Herrera JE, Hock R, Scheer U, Bustin M 1997 Clusters of nucleosomes containing chromosomal protein HMG-17 in chromatin. J Mol Biol 274:454-465
35. Landsman D, Bustin M 1986 Chromosomal proteins HMG-14 and HMG-17. Distinct multigene families coding for similar types of transcripts. J Biol Chem 261:16087-16091
36. Prymakowska-Bosak M, Misteli T, Herrera JE, Shirakawa H, Birger Y, Garfield S, Bustin M 2001 Mitotic phosphorylation prevents the binding of HMGN proteins to chromatin. Mol Cell Biol 21:5169-5178
37. Ueda T, Postnikov YV, Bustin M 2006 Distinct domains in high mobility group N variants modulate specific chromatin modifications. J Biol Chem 281:10182-10187
38. Plotnikov A, Varghese B, Tran TH, Liu C, Rui H, Fuchs SY 2009 Impaired turnover of prolactin receptor contributes to transformation of human breast cells. Cancer Res 69:3165-3172
39. Conway-Campbell BL, Brooks AJ, Robinson PJ, Perani M, Waters MJ 2008 The extracellular domain of the growth hormone receptor interacts with coactivator activator to promote cell proliferation. Mol Endocrinol 22:2190-2202
40. Ihle JN, Kerr IM 1995 Jaks and Stats in signaling by the cytokine receptor superfamily. Trends Genet 11:69-74
41. Boutin JM, Jolicoeur C, Okamura H, Gagnon J, Edery M, Shirota M, Banville D, Dusanter-Fourt I, Djiane J, Kelly PA 1988 Cloning and expression of the rat prolactin receptor, a member of the growth hormone/prolactin receptor gene family. Cell 53:69-77
42. Liao HJ, Carpenter G 2007 Role of the Sec61 translocon in EGF receptor trafficking to the nucleus and gene expression. Mol Biol Cell 18:1064-1072
43. Nilsson J, Bjursell G, Kannius-Janson M 2006 Nuclear Jak2 and transcription factor NF1-C2: a novel mechanism of prolactin signaling in mammary epithelial cells. Mol Cell Biol 26:5663-5674
44. Lebrun JJ, Ali S, Ullrich A, Kelly PA 1995 Proline-rich sequence-mediated Jak2 association to the prolactin receptor is required but not sufficient for signal transduction. J Biol Chem 270:10664-10670
45. Clevenger CV, Furth PA, Hankinson SE, Schuler LA 2003 The role of prolactin in mammary carcinoma. Endocr Rev 24:1-27
46. Lincoln DT, Sinowatz F, Temmim-Baker L, Baker HI, Kolle S, Waters MJ 1998 Growth hormone receptor expression in the nucleus and cytoplasm of normal and neoplastic cells. Histochem Cell Biol 109:141-159
47. Ueda T, Furusawa T, Kurahashi T, Tessarollo L, Bustin M 2009 The nucleosome binding protein HMGN3 modulates the transcription profile of pancreatic beta cells and affects insulin secretion. Mol Cell Biol 29:5264-5276

48. Rascle A, Lees E 2003 Chromatin acetylation and remodeling at the Cis promoter during STAT5-induced transcription. Nucleic Acids Res 31:6882-6890
49. Trieschmann L, Martin B, Bustin M 1998 The chromatin unfolding domain of chromosomal protein HMG-14 targets the N-terminal tail of histone H3 in nucleosomes. Proc Natl Acad Sci U S A 95:5468-5473
50. Alfonso PJ, Crippa MP, Hayes JJ, Bustin M 1994 The footprint of chromosomal proteins HMG-14 and HMG-17 on chromatin subunits. J Mol Biol 236:189-198
51. Huo L, Wang YN, Xia W, Hsu SC, Lai CC, Li LY, Chang WC, Wang Y, Hsu MC, Yu YL, Huang TH, Ding Q, Chen CH, Tsai CH, Hung MC 2010 RNA helicase A is a DNA-binding partner for EGFR-mediated transcriptional activation in the nucleus. Proc Natl Acad Sci U S A 107:16125-16130
52. Beguelin W, Diaz Flaque MC, Proietti CJ, Cayrol F, Rivas MA, Tkach M, Rosemblit C, Tocci JM, Charreau EH, Schillaci R, Elizalde PV 2010 Progesterone receptor induces ErbB-2 nuclear translocation to promote breast cancer growth via a novel transcriptional effect: ErbB-2 function as a coactivator of Stat3. Mol Cell Biol 30:5456-5472
53. Razandi M, Pedram A, Greene GL, Levin ER 1999 Cell membrane and nuclear estrogen receptors (ERs) originate from a single transcript: studies of ERalpha and ERbeta expressed in Chinese hamster ovary cells. Mol Endocrinol 13:307-319
54. Lee TI, Johnstone SE, Young RA 2006 Chromatin immunoprecipitation and microarray-based analysis of protein location. Nat Protoc 1:729-748
55. Nelson JD, Denisenko O, Bomsztyk K 2006 Protocol for the fast chromatin immunoprecipitation (ChIP) method. Nat Protoc 1:179-185
56. Zhu N, Hansen U 2007 HMGN1 modulates estrogen-mediated transcriptional activation through interactions with specific DNA-binding transcription factors. Mol Cell Biol 27:8859-8873
57. Fang F, Rycyzyn MA, Clevenger CV 2009 Role of c-Myb during prolactin-induced signal transducer and activator of transcription 5a signaling in breast cancer cells. Endocrinology 150:1597-1606
58. Fang F, Zheng J, Galbaugh TL, Fiorillo AA, Hjort EE, Zeng X, Clevenger CV 2010 Cyclophilin B as a co-regulator of prolactin-induced gene expression and function in breast cancer cells. J Mol Endocrinol 44:319-329
59. Galbaugh T, Feeney Y, Clevenger CV 2010 Prolactin Receptor-Integrin Crosstalk Mediated by SIRP{alpha} in Breast Cancer Cells. Mol Cancer Res

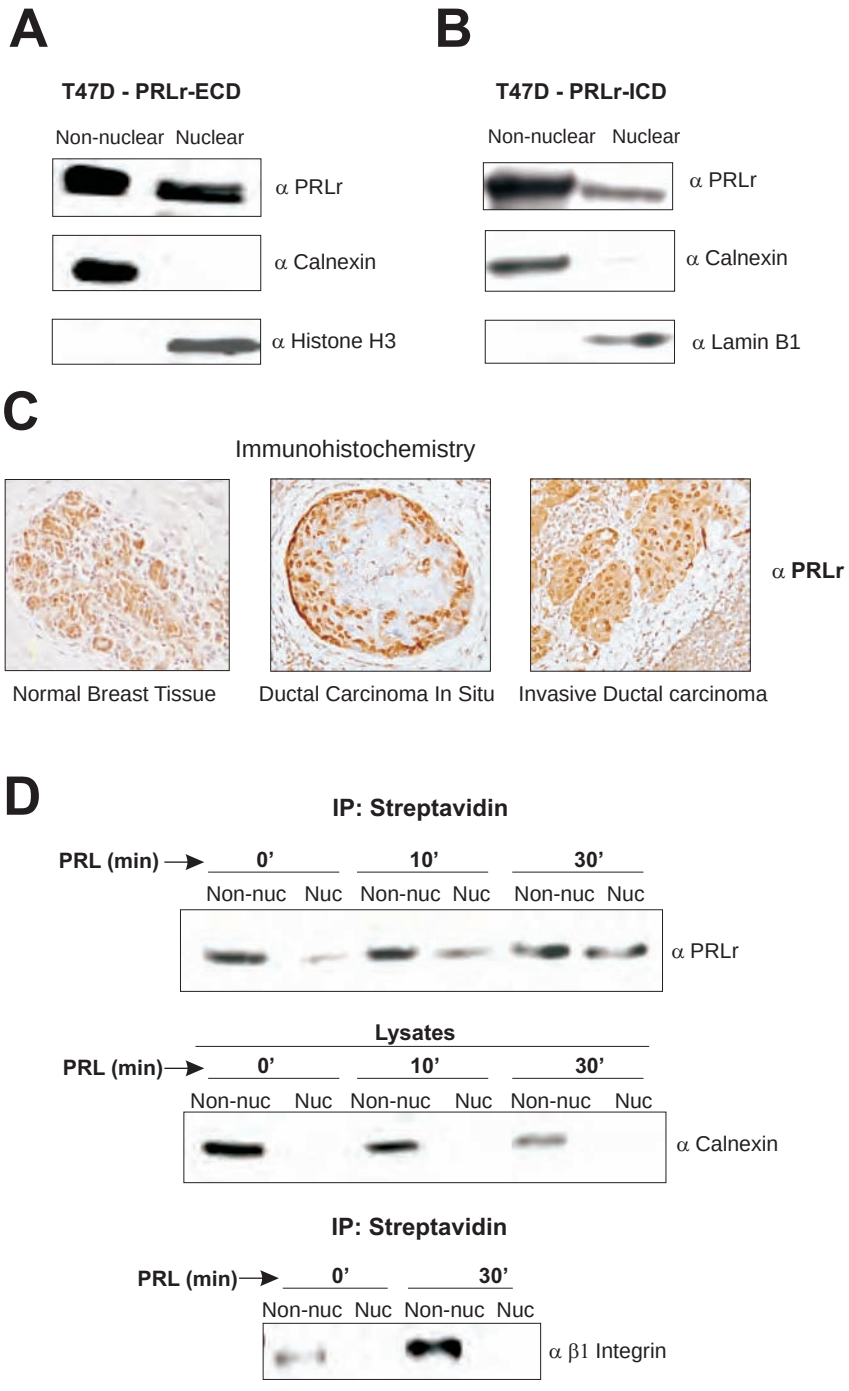
A
T47D - PRLr-ECD
Non-nuclear Nuclear
α PRLr
α Calnexin
α Histone H3
B
T47D - PRLr-ICD
Non-nuclear Nuclear
α PRLr
α Calnexin
α Lamin B1
C
Immunohistochemistry
α PRLr
Normal Breast Tissue
Ductal Carcinoma In Situ
Invasive Ductal carcinoma
D
IP: Streptavidin
PRL (min)
0'
10'
30'
Non-nuc Nuc Non-nuc Nuc Non-nuc Nuc
α PRLr
Lysates
PRL (min)
0'
10'
30'
Non-nuc Nuc Non-nuc Nuc Non-nuc Nuc
α Calnexin
IP: Streptavidin
PRL (min)
0'
30'
Non-nuc Nuc Non-nuc Nuc
α β1 Integrin

Fig 1

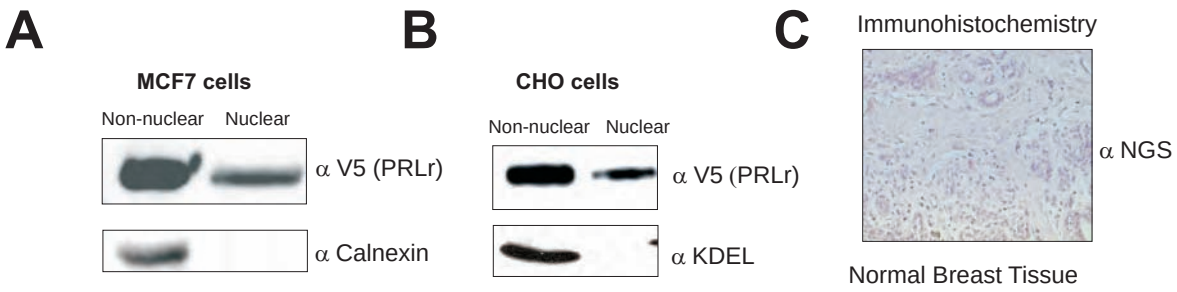
A
MCF7 cells
Non-nuclear
Nuclear
α V5 (PRLr)
α Calnexin
B
CHO cells
Non-nuclear
Nuclear
α V5 (PRLr)
α KDEL
C
Immunohistochemistry
α NGS
Normal Breast Tissue

Fig S1

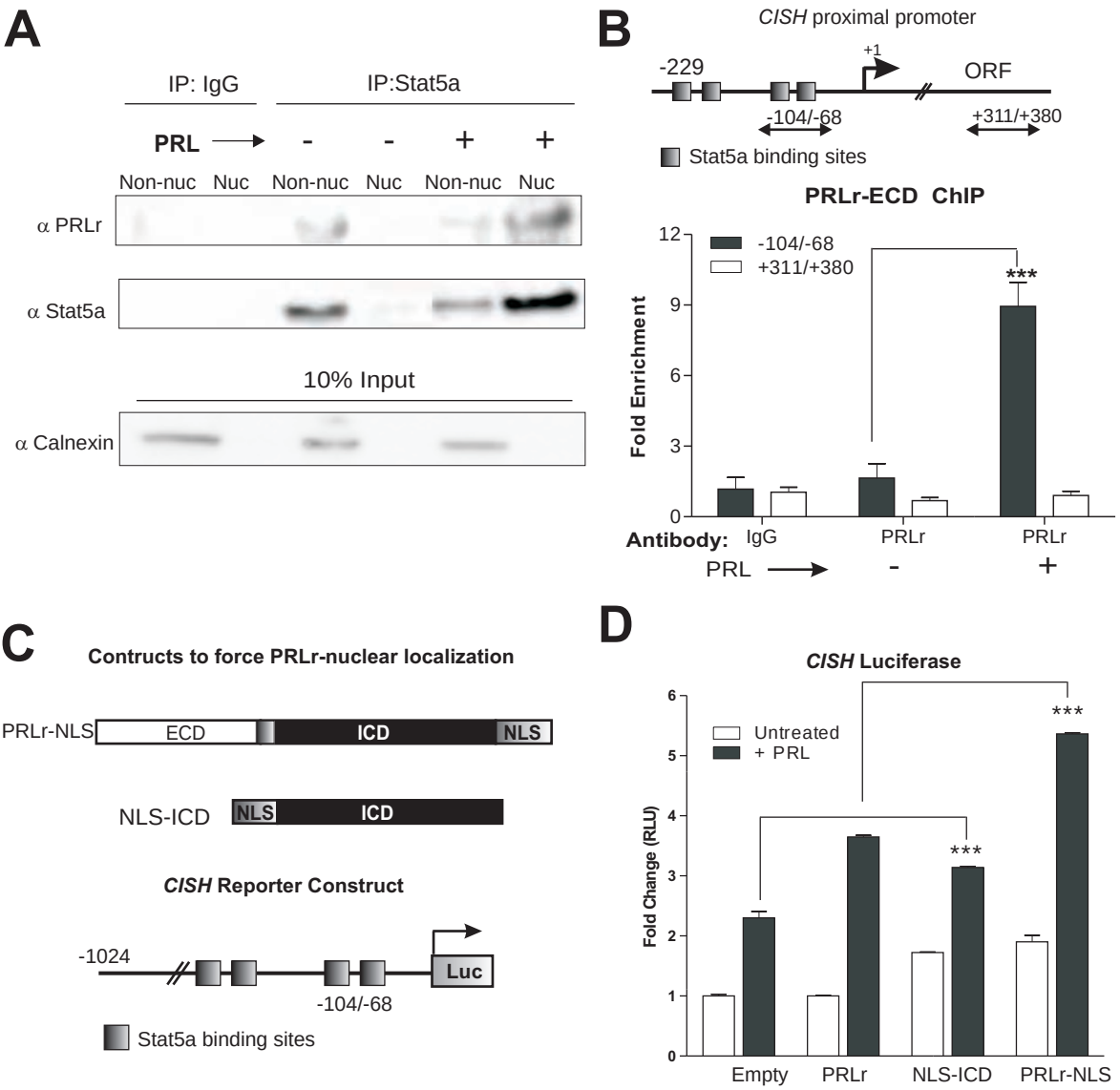
A
IP: IgG
IP:Stat5a
PRL
- - + +
Non-nuc Nuc Non-nuc Nuc Non-nuc Nuc
α PRLr
α Stat5a
10% Input
α Calnexin
B
CISH proximal promoter
-229
+1
ORF
-104/-68
+311/+380
Stat5a binding sites
PRLr-ECD ChIP
-104/-68
+311/+380
***
Fold Enrichment
12
9
6
3
0
Antibody: IgG PRLr PRLr
PRL - +
C
Contructs to force PRLr-nuclear localization
PRLr-NLS
ECD
ICD
NLS
NLS-ICD
NLS
ICD
CISH Reporter Construct
-1024
Luc
-104/-68
Stat5a binding sites
D
CISH Luciferase
Untreated
+ PRL
***
***
Fold Change (RLU)
6
5
4
3
2
1
0
Empty PRLr NLS-ICD PRLr-NLS

Fig 2

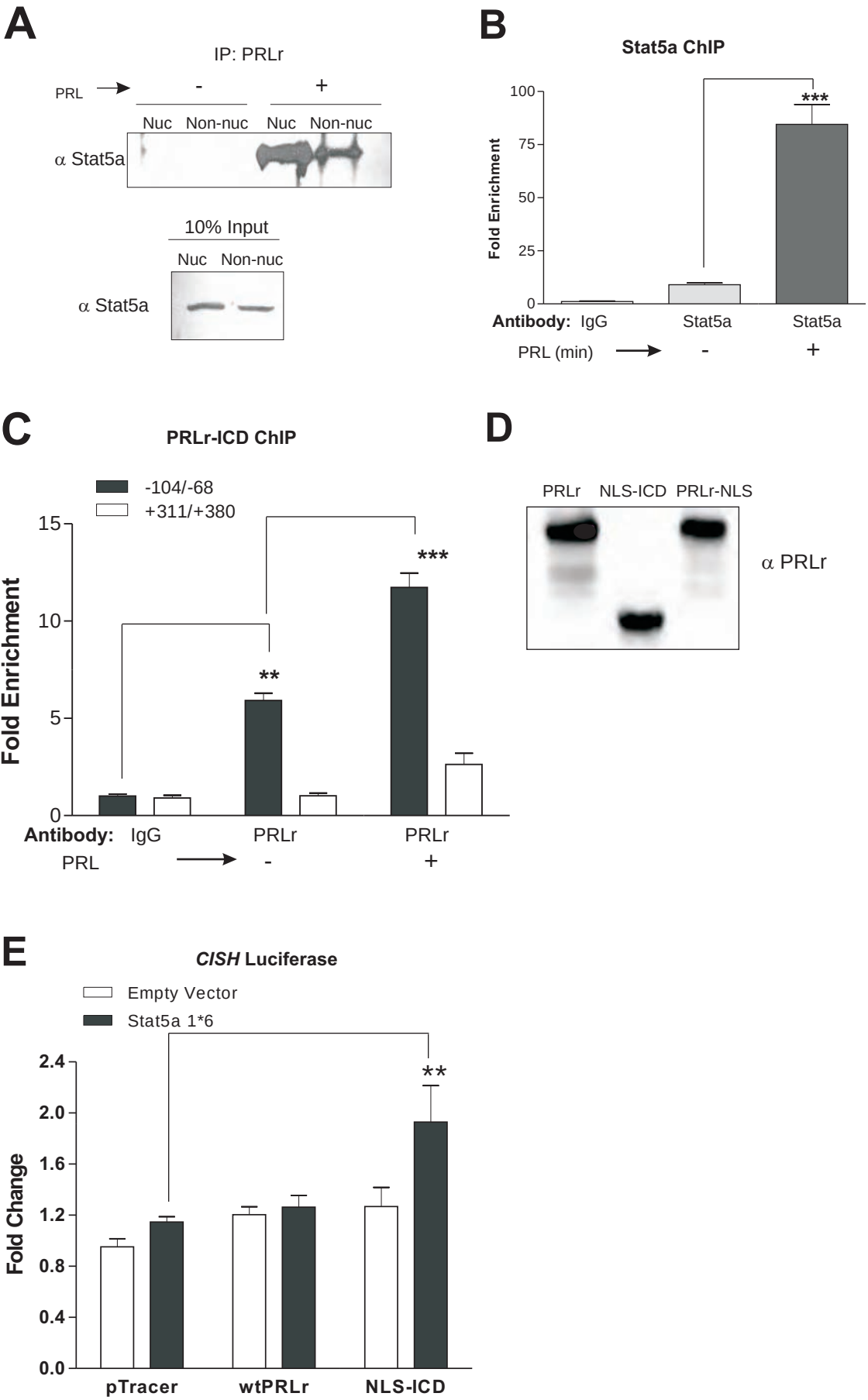
A
IP: PRLr
PRL
-
+
Nuc Non-nuc Nuc Non-nuc
α Stat5a
10% Input
Nuc Non-nuc
α Stat5a
B
Stat5a ChIP
Fold Enrichment
100
75
50
25
0
***
Antibody: IgG Stat5a Stat5a
PRL (min)
-
+
C
PRLr-ICD ChIP
-104/-68
+311/+380
Fold Enrichment
15
10
5
0
**
***
Antibody: IgG PRLr PRLr
PRL
-
+
D
PRLr NLS-ICD PRLr-NLS
α PRLr
E
CISH Luciferase
Empty Vector
Stat5a 1*6
Fold Change
2.4
2.0
1.6
1.2
0.8
0.4
0.0
**
pTracer wtPRLr NLS-ICD

Fig S2

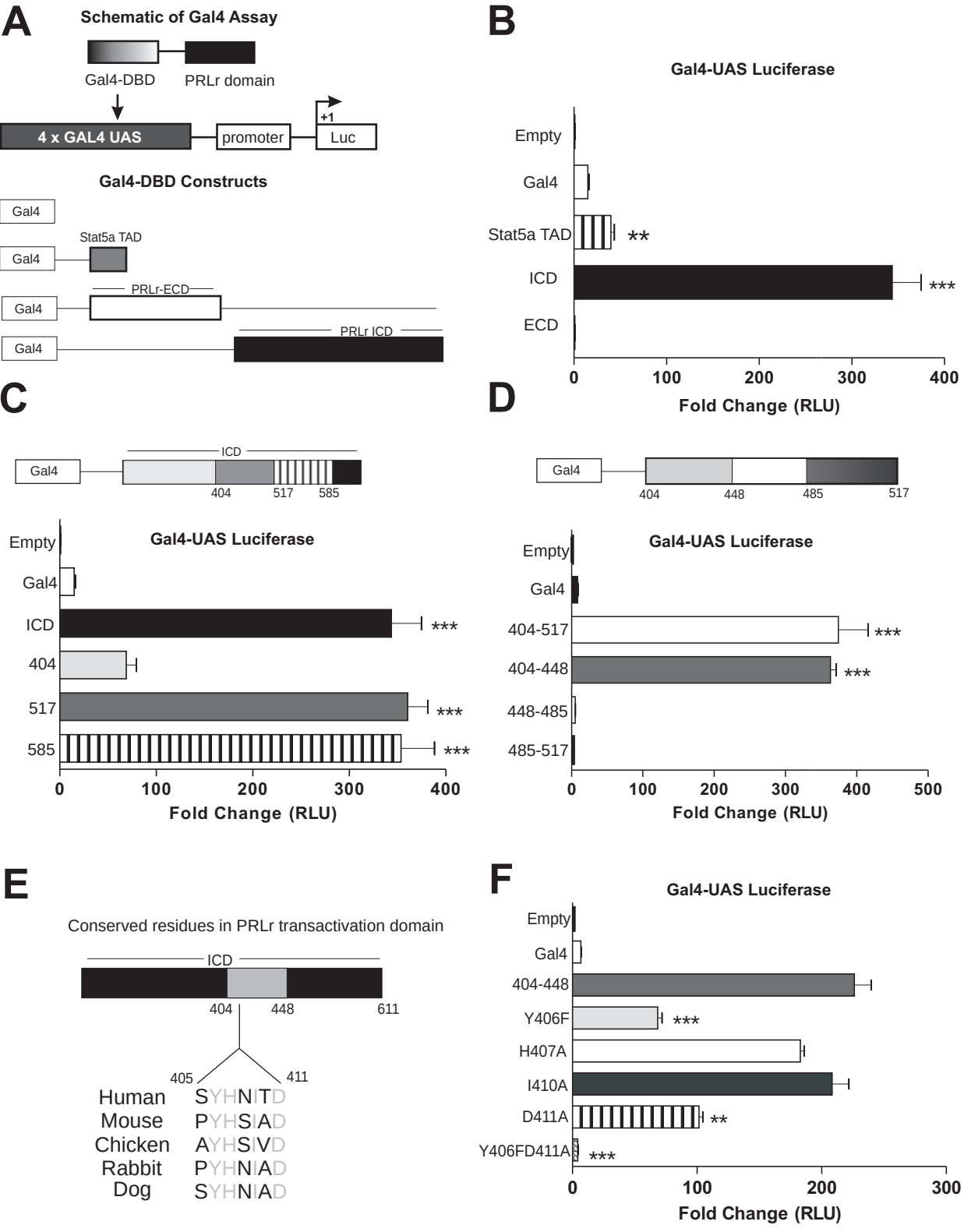
A
Schematic of Gal4 Assay
Gal4-DBD
PRLr domain
4 x GAL4 UAS
promoter
+1
Luc
Gal4-DBD Constructs
Gal4
Stat5a TAD
PRLr-ECD
PRLr ICD
B
Gal4-UAS Luciferase
Empty
Gal4
Stat5a TAD
ICD
ECD
**
***
0
100
200
300
400
Fold Change (RLU)
C
ICD
404
517
585
Gal4-UAS Luciferase
Empty
Gal4
ICD
404
517
585
***
0
100
200
300
400
Fold Change (RLU)
D
Gal4
404
448
485
517
Gal4-UAS Luciferase
Empty
Gal4
404-517
404-448
448-485
485-517
***
0
100
200
300
400
500
Fold Change (RLU)
E
Conserved residues in PRLr transactivation domain
ICD
404
448
611
405
411
Human SYHNITD
Mouse PYHSIAD
Chicken AYHSIVD
Rabbit PYHNIAD
Dog SYHNIAD
F
Gal4-UAS Luciferase
Empty
Gal4
404-448
Y406F
H407A
I410A
D411A
Y406FD411A
***
**
0
100
200
300
Fold Change (RLU)

Fig 3

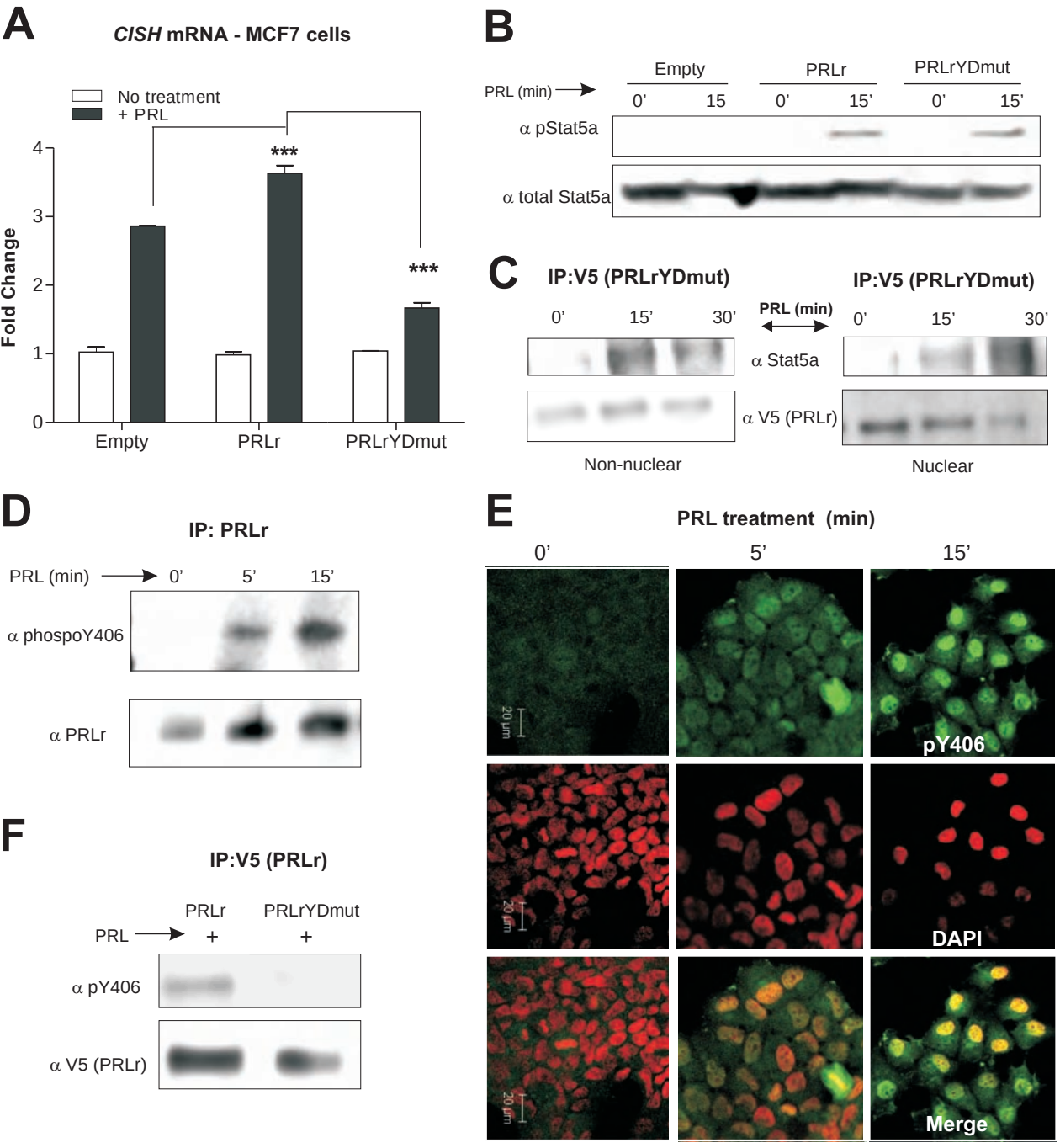
A
CISH mRNA - MCF7 cells
No treatment
+ PRL
Fold Change
***
***
Empty
PRLr
PRLrYDmut
B
PRL (min)
Empty
PRLr
PRLrYDmut
0’
15
0’
15’
0’
15’
α pStat5a
α total Stat5a
C
IP:V5 (PRLrYDmut)
IP:V5 (PRLrYDmut)
0’
15’
30’
PRL (min)
0’
15’
30’
α Stat5a
α V5 (PRLr)
Non-nuclear
Nuclear
D
IP: PRLr
PRL (min)
0’
5’
15’
α phospoY406
α PRLr
E
PRL treatment (min)
0’
5’
15’
20 µm
pY406
DAPI
Merge
F
IP:V5 (PRLr)
PRLr
PRLrYDmut
PRL
+
+
α pY406
α V5 (PRLr)

Fig 4

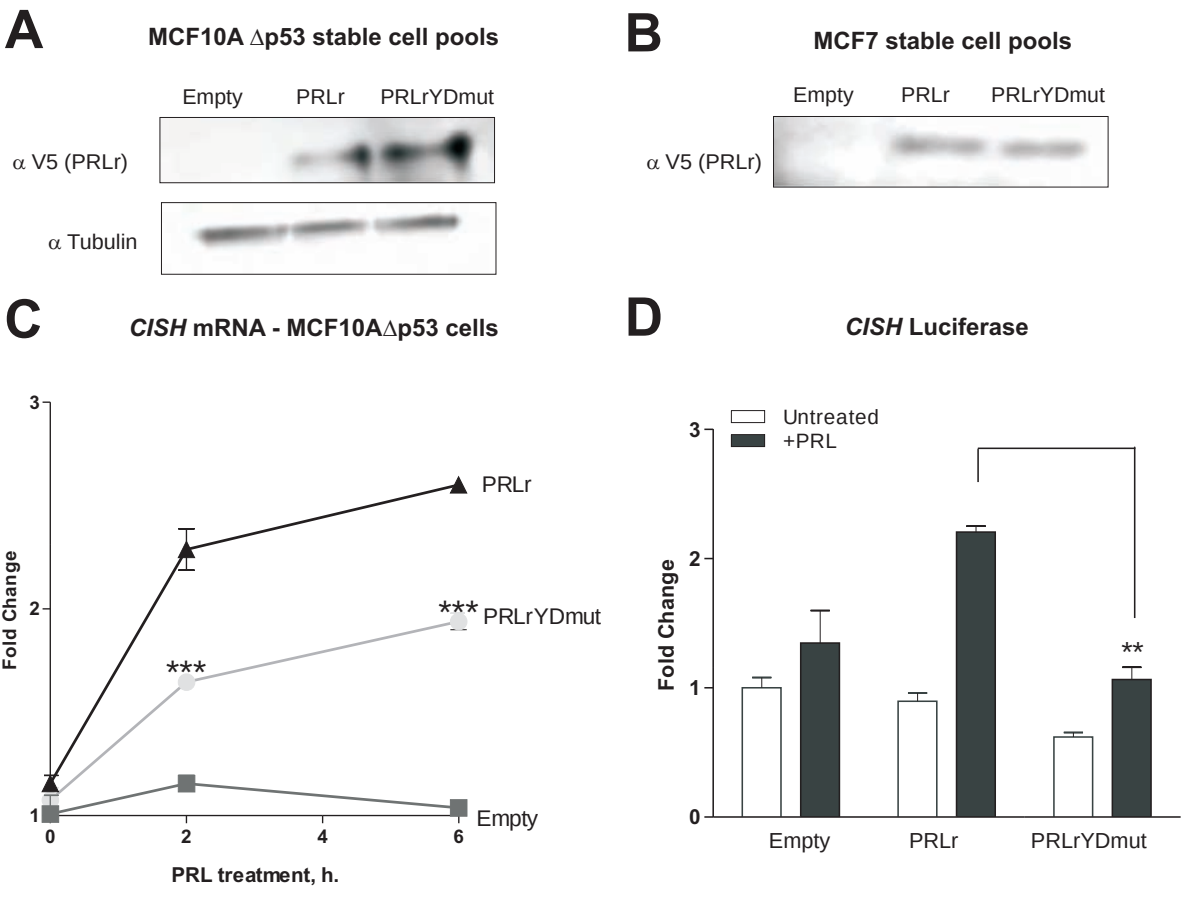
A
MCF10A Δp53 stable cell pools
Empty
PRLr
PRLrYDmut
α V5 (PRLr)
α Tubulin
B
MCF7 stable cell pools
Empty
PRLr
PRLrYDmut
α V5 (PRLr)
C
CISH mRNA - MCF10AΔp53 cells
Fold Change
PRLr
PRLrYDmut
Empty
***
***
PRL treatment, h.
D
CISH Luciferase
Untreated
+PRL
Fold Change
**
Empty
PRLr
PRLrYDmut
E
PRLr
PRLrYDmut
PRL (min)
0'
15'
30'
0'
15'
30'
α pAkt
α total Akt
α pErk
α total Erk

Fig S3

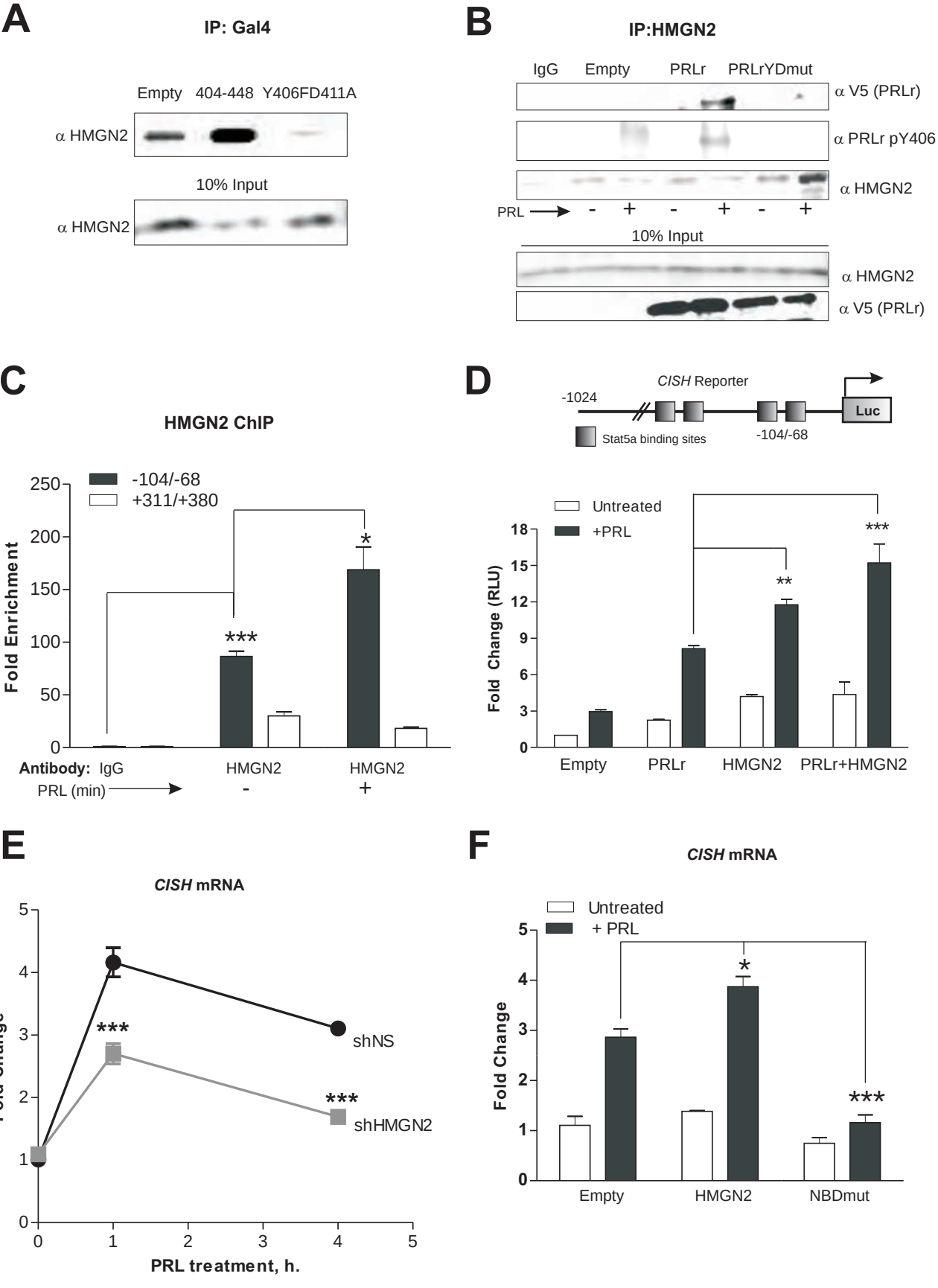
A
IP: Gal4
Empty
404-448
Y406FD411A
α HMGN2
10% Input
α HMGN2
B
IP:HMGN2
IgG
Empty
PRLr
PRLrYDmut
α V5 (PRLr)
α PRLr pY406
α HMGN2
PRL
- + - + - +
10% Input
α HMGN2
α V5 (PRLr)
C
HMGN2 ChIP
-104/-68
+311/+380
Fold Enrichment
250
200
150
100
50
0
***
*
Antibody: IgG
HMGN2
HMGN2
PRL (min)
-
+
D
CISH Reporter
-1024
Luc
Stat5a binding sites
-104/-68
Untreated
+PRL
Fold Change (RLU)
18
15
12
9
6
3
0
***
**
Empty
PRLr
HMGN2
PRLr+HMGN2
E
CISH mRNA
Fold Change
5
4
3
2
1
0
***
***
shNS
shHMGN2
0
1
2
3
4
5
PRL treatment, h.
F
CISH mRNA
Untreated
+ PRL
Fold Change
5
4
3
2
1
0
*
***
Empty
HMGN2
NBDmut

Fig 5

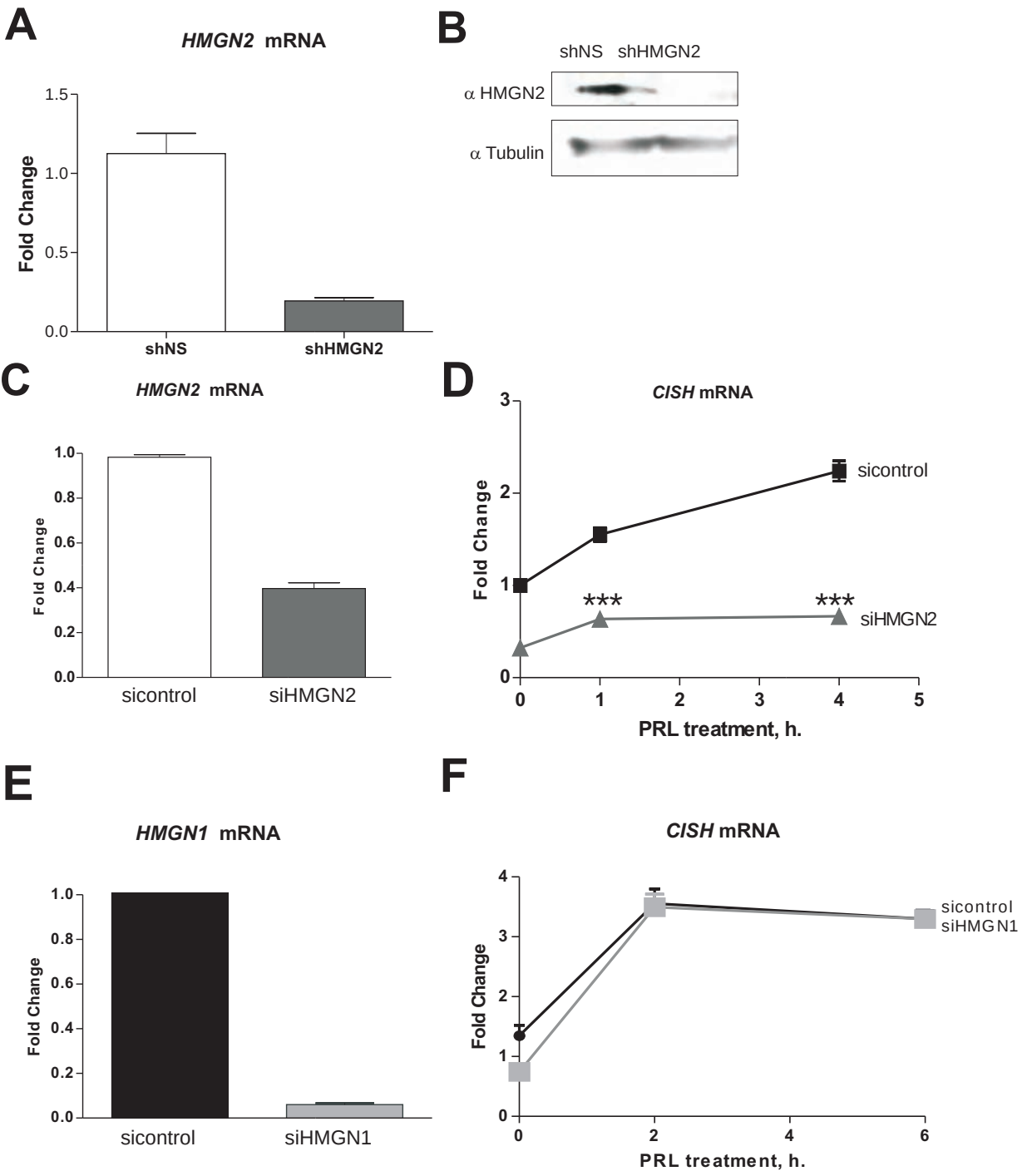
A
HMGN2 mRNA
Fold Change
1.5
1.0
0.5
0.0
shNS
shHMGN2
B
shNS shHMGN2
α HMGN2
α Tubulin
C
HMGN2 mRNA
Fold Change
1.0
0.8
0.6
0.4
0.2
0.0
sicontrol
siHMGN2
D
CISH mRNA
Fold Change
3
2
1
0
***
***
sicontrol
siHMGN2
0
1
2
3
4
5
PRL treatment, h.
E
HMGN1 mRNA
Fold Change
1.0
0.8
0.6
0.4
0.2
0.0
sicontrol
siHMGN1
F
CISH mRNA
Fold Change
4
3
2
1
0
sicontrol
siHMGN1
0
2
4
6
PRL treatment, h.

Fig S4

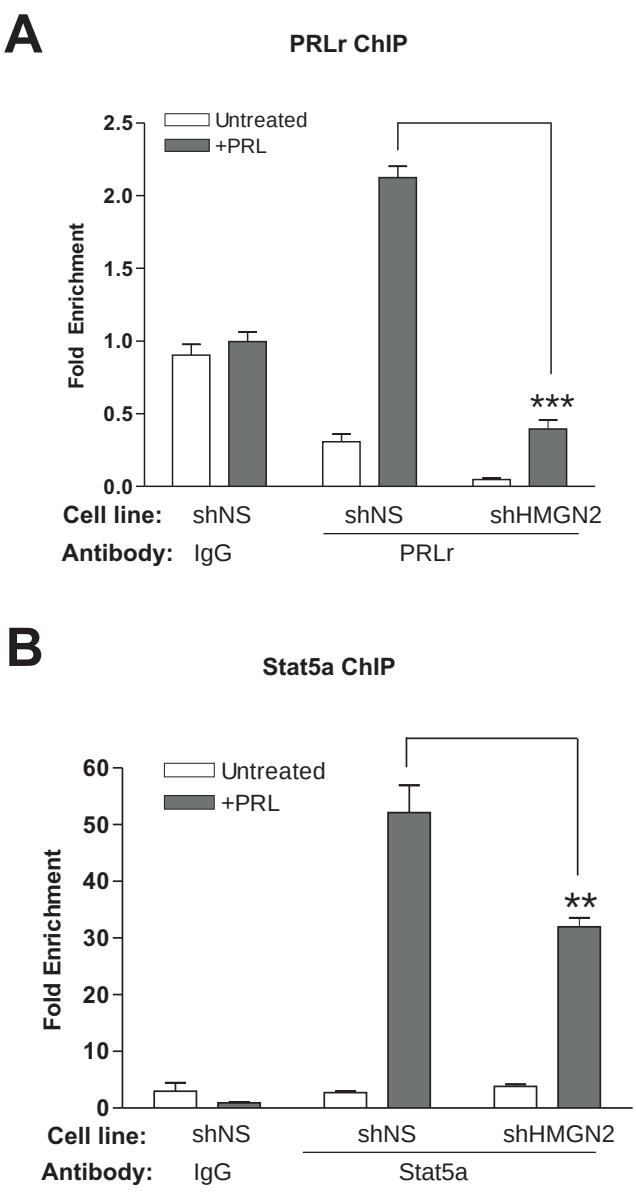
A
PRLr ChIP
Untreated
+PRL
Fold Enrichment
2.5
2.0
1.5
1.0
0.5
0.0
***
Cell line: shNS shNS shHMGN2
Antibody: IgG PRLr
B
Stat5a ChIP
Untreated
+PRL
Fold Enrichment
60
50
40
30
20
10
0
**
Cell line: shNS shNS shHMGN2
Antibody: IgG Stat5a

Fig 6

A

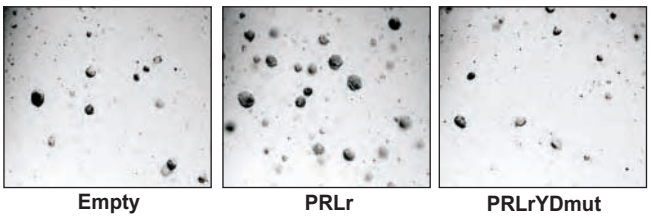
Empty
PRLr
PRLrYDmut

B

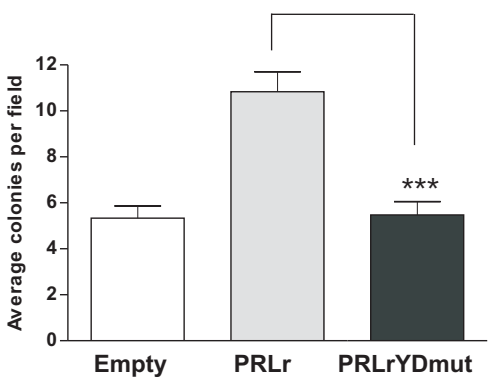
Average colonies per field
12
10
8
6
4
2
0
***
Empty
PRLr
PRLrYDmut

Fig 7

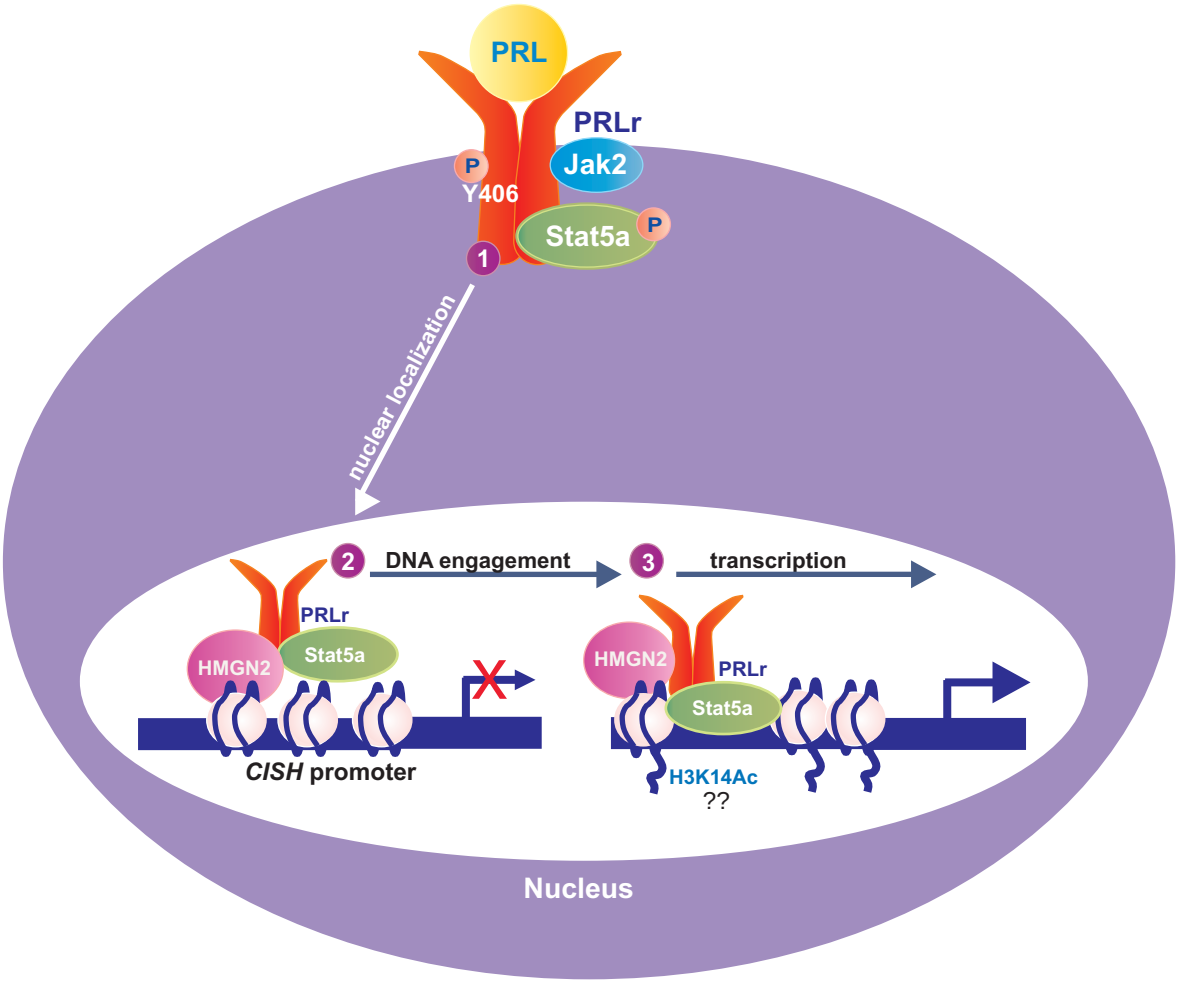
PRL
PRLr
Jak2
P
Y406
Stat5a
P
1
nuclear localization
2
DNA engagement
3
transcription
PRLr
HMGN2
Stat5a
CISH promoter
HMGN2
PRLr
Stat5a
H3K14Ac
??
Nucleus

Fig 8